INRIA

INSTITUT NATIONAL DE RECHERCHE EN INFORMATIQUE ET EN AUTOMATIQUE

Towards biologically plausible regularization mechanisms

T. Viéville,

N° 4965

Octobre 2003

THÈME 3

ISSN 0249-6399 ISRN INRIA/RR--4965--FR+ENG

INRIA
SOPHIA ANTIPOLIS

Towards biologically plausible regularization mechanisms

T. Viéville*,

Thème 3 — Interaction homme-machine,
images, données, connaissances
Projet Odyssee

Rapport de recherche n° 4965 — Octobre 2003 — 39 pages

Abstract: This study aims at proposing an implementation of regularization mechanisms compatible with biological operators. More precisely, cortical maps code vectorial parametric quantities, computed by network of neurons.

One of these methods is based on an integral approximation of the diffusion operator used in regularization mechanisms. Following this formulation, the present development defines an optimal implementation of such an integral operator with the interesting property that, when used as a model of biological plausible mechanisms, it corresponds to a simple local feedback defined over a small bounded region of the parametric space.

This formalism also allows to develop the case of several cortical maps in interaction. We propose simple biologically inspired conditions to guaranty the stability of such interactions.

As such it may be linked to what is processed in a cortical column of the brain and provides a biological plausible model of cortical maps computation: here feedbacks between related cortical maps are discussed.

Key-words: Regularization methods, Cortical feedback mechanisms, Coupling between cortical maps

* http://www.inria.fr/Thierry.Vieville

Unité de recherche INRIA Sophia Antipolis
2004, route des Lucioles, BP 93, 06902 Sophia Antipolis Cedex (France)
Téléphone : +33 4 92 38 77 77 — Télécopie : +33 4 92 38 77 65

Vers des mécanismes de régularisation biologiquement plausibles

Résumé : Cette étude propose une implémentation de mécanismes de régularisation compatibles avec les opérateurs biologiques. Plus précisément, les cartes corticales codes des quantités vectorielles, calculées par des réseaux de neurones. En vision par ordinateur, des quantités similaires sont calculées efficacement en utilisant une implémentation d'équations aux dérivées partielles qui définissent des processus de régularisation, permettant d'obtenir une estimation bien définies de ces quantités.

Une de ces méthodes est basée sur l'approximation intégrale des opérateurs de diffusion utilisés dans les mécanismes de régularisation. En suivant cette formulation, the présent développement définit une implémentation oprimale de ces opérateurs intégraux avec la propriété intéressante que, lors de son utilisation en tant que modèle biologiquement plausible, il correspond a un simple mécanisme de rétroaction sur un région bornée autour du point à estimr.

Ce formalisme permet aussi de considérer le cas de plusieurs cartes corticales en interaction. Nous proposons, sur la base de simples considérations biologiques, des conditions qui garantissent la stabilité de telles interactions.

Ce mécanisme peut-être relié au calcul effectué au sein d'une colonne corticale du cerveau et induit un modèle biologiquement plausible du calcul au sein des cartes corticles: ici les mécanismes de rétroaction entre différentes cartes corticales sont discutés.

Mots-clés : Méthodes de régularisation, Mécanismes corticaux de régularisation, Couplage entre cartes corticales.

1 Introduction

Cortical maps

Perceptual processes, in computer or biological vision, require the computation of "maps" of quantitative values. The retinal image itself is a "retinotopic map": for each cell of the retina or each pixel of the image, there is a value corresponding to the image intensity at this location. This is a vectorial value for color images. A step further, in early-vision, the retinal image contrast is computed at each location, allowing to detect image edges related to boundaries between image areas. Such maps encode not only the contrast magnitude, but several other cues: contrast orientation related to edge orientation, shape curvature, binocular disparity related to the visual depth, color cues, temporal disparity between two consecutive images in relation with visual motion detection, etc.. There are such detectors in both artificial visual systems (see e.g. [16] for a general introduction) and in the brain neuronal structures involved in vision perception (see e.g. [33] for a classical overview). Such maps are not only parameterized by retinotopic locations, but also 3D locations, or parameterized by other parameters such as orientation, retinal velocity, etc..

Both systems have to solve the same perceptual tasks and very likely make the same kind of hypotheses about the observed surroundings: they share the same models. It is thus a relevant challenge to elaborate common theorical tools in both fields, considering neuro-science models and artificial vision algorithms.

The Partial Differential Equation (PDE) approach

In computer vision, a relevant and efficient theory is now available regarding the definition and computation of such maps of quantitative values (see e.g. [1] for a didactic introduction about the "axiomatization" of this part of computer vision). This formalism not only provides a clear basic of "what is to be done" (i.e. requirements in order to have coherent and consistent definitions) but also of "how to do it" since the theory is effective in the sense that efficient implementations may be derived (see e.g. [3] for a recent treatise on this subject). The "what is to be done" level is formalized in terms of a criterion to minimize and the "how to do it" level is related to the, so called, Euler-

Lagrange equations which allow to improve an initial guess of the solution and get closer to the optimal solution. At a technical level, as revisited in this paper, these quantities are efficiently computed using implementations of partial differential equations which define regularization processes allowing to obtain well-defined estimations of these quantities. This powerful methodology is also very general in the sense that a large variety of computational problems are solvable within this framework (see e.g. [13, 12] for a review).

A step further, PDE calculations regularize their input, i.e. provide a well-defined and stable estimation even in the case of noisy or partially defined data. Thanks to this property, algorithms have performances closer to those of biological systems, than those of usual artificial neuronal networks.

Using Neuronal Network (NN) models

In biological vision modeling, the situation is dominated by the idea that "cortical maps code vectorial parametric quantities are computed by network of neurons" (e.g. [23] for a recent review). Such models allow to analyze in details the biological substrate of such computations (e.g. [14]), in other words to raise efficient hypotheses about "how it is done". Such models are either based on some "ad-hoc" mechanisms, more precisely specific descriptions of neuronal connections which are "plausible" regarding one or another operation (e.g. [33] for edge and disparity calculations) or more abstract mechanisms (e.g. [40, 58] where a computational description of early-vision and motion computations in terms of adaptive linear filtering is proposed). Biological models which formalize the "what is to be done" aspect (e.g [18]) are not directly linked to the previous ones. Although these approaches already allow a deep understanding of what is processed in important areas of the brain, including computer simulations [24],there is no clear link with the computer vision algorithms mentioned before.

Building a link between PDE and NN

Such a link, would indeed have several advantages, providing a methodology to relate the "what is to be done" and the "how to do it" levels and also providing a very general computational framework for such calculations. Furthermore,

this link will provide a "common framework" between computational and biological vision in order to develop common models and biological plausible algorithms. However, building such a link is not immediate because there is yet no clear understanding of how such complex differential non-linear methods could correspond to neuronal mechanisms although the question has been already raised [15, 46, 36].

Implementing PDE as NN

In order to build this link, we must have a method which allows to implement the computer vision partial differential equations, using networks of neuronal units. As it will made explicit in the sequel, the difficult point is the anisotropic diffusion operators implementation. Concretely, such mechanisms must integrate the information in a bounded neighborhood so that the cooperation between these units allow a global computation of the quantitative map. Furthermore, to be biologically plausible, such mechanisms must be based on simple local linear feedback [14, 23]. In other words, we must provide a "particle implementation" of such numerical computations. Such a method, used in fluid dynamics computation has been introduced by Leonard [37] followed by Raviat and Mas-Gallic [50] and developed by Degond and Mas-Gallic [11]. It is based on an integral approximation of the diffusion operator used in the regularization mechanism.

The goal of this paper is, following this track, to describe how computer vision partial differential equations can be implemented using biologically plausible networks of neuronal units.

What is the paper about[2]

In the next section, we revisit the computer vision partial differential equation methodology in the case of vectorial maps and re-derive an improved version of the Degond and Mas-Gallic method, considering an optimal implementation of such an integral operator with the interesting property that when used as

[2] **About footnotes** Since this paper presents material from both computer science and life science, we have introduced several footnotes reviewing basic facts on both sizes, providing the reader with a self-content document.

a model of biological plausible mechanisms, it corresponds to a simple local feedback defined over a small bounded region inside the parametric space.

This formalism also allows to develop the case of several cortical maps in interaction. We propose a simple condition to guaranty the stability of such interacting layers.

We finally will illustrate this framework considering some examples of cortical maps computations, discussing the role of feedbacks.

In particular, we verify that under biological assumptions, cortical map interactions in our framework is a well-defined and convergent process.

Notations We write *vectors* and *matrices* in bold letters, matrices being written with capital letters and scalars in italic. The dual of a quantity $\mathbf{x}$ is represented as its transpose $\mathbf{x}^T$, the dot-product between vectors being written $\mathbf{x}^T\mathbf{y}$. We represent the components of a vector using superscripts, e.g.: $\mathbf{x} = (x^0, x^1, x^2)^T$.

Similarly we write *tensors* in bold letters with covariant and contravariant indexes written as indices and exponent, respectively. For instance, the following *Kronecker* symbol $\delta_i^j =$ if $i = j$ then 1 else 0, has covariant index i and contravariant index j. In this context, a $m \times n$ matrix $M_i^j, i = 1..n, j = 1..m$ is a 1-covariant / 1 -contravariant tensor. Although, the "Einstein" notation allows implicit summations of tensor indexes, it appears clearer, here, to explicit these summations.

For vector of integer indices $\alpha = (\alpha_1 \cdots \alpha_n) \in \mathcal{N}^n$ we write:

$$|\alpha| = \alpha_1 + \cdots + \alpha_n \text{ and } \alpha! = \alpha_1! \cdots \alpha_n!$$

so that we can write concisely:

$$\mathbf{x}^\alpha = x_1^{\alpha_1} \cdots x_n^{\alpha_n} \text{ and } \partial_{\mathbf{x}}^\alpha f = \frac{\partial^{|\alpha|} f}{\partial x_1^{\alpha_1} \ldots \partial x_n^{\alpha_n}}$$

while the Taylor expansion of a function $h : \mathcal{R}^n \to \mathcal{R}$ becomes:

$$h(\mathbf{x}) = h(\mathbf{x}_0) + \sum_{|\alpha|=1}^{r} \frac{\partial^\alpha h}{\alpha!} (\mathbf{x} - \mathbf{x}_0)^\alpha + R^r h$$

where the remainder $R^\epsilon h$ may be written using an integral form[3].

[3] Here:

$$R^r h = \sum_{|\alpha|=r+1} \frac{r+1}{\alpha!} \int_{[0,1]} (\mathbf{x} - \mathbf{x}_0)^\alpha (1-u)^r \, \partial^\alpha h(\mathbf{x}_0 + u(\mathbf{x} - \mathbf{x}_0)) \, du$$

If the support is included in a ball of radius ϵ, the remainder is bounded by the standard condition:

$$||R^r \mathbf{h}||_{0,\infty} < C \, \epsilon^{r-1} ||\mathbf{h}||_{r+1,\infty}$$

2 Using anisotropic diffusion operators.

Let us briefly revisit the computer vision partial differential equation methodology in the case of Euclidean vectorial maps (how it can be generalized to non-Euclidean cortical maps[4] computations and how a general class of non-linear diffusion operators are implemented within the present frameworks is discussed elsewhere [66]). The goal of this section is to introduce this approach and point out where is the key problem in terms of biological plausibility.

Here, as required in some situations (e.g. [1, 12, 29]), we consider functions which values are not scalars but vectors.

Defining a cortical map function from a criterion. Let us consider a vectorial map:

$$\mathbf{h} : \mathcal{R}^n \rightarrow \mathcal{R}^m$$

with a "reference" function $\bar{\mathbf{h}}(\mathbf{x})$ related to an input or measure $\mathbf{m}(\mathbf{x})$, as schematized in Fig. 1.

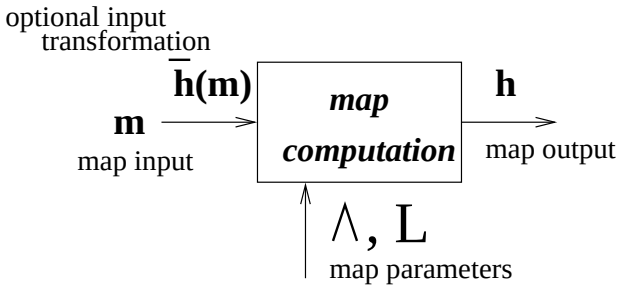

Figure 1: Input/output scheme of regularization process, see text for details.

where C is a fixed quantity while

$$||f||_{s,\infty} = \sup_{0 \geq k \geq s} \left[\text{sup ess}_{|\alpha|=k,\, \mathbf{x} \in \mathcal{R}^n} |\partial^\alpha f(\mathbf{x})| \right] .$$

[4]Generalization from $\mathcal{R}^n$ to non-linear manifolds is also to be considered because cortical maps are intrinsically "curved space" with the fact that parametric spaces of dimension $n \geq 2$ (e.g. the visual areas which code retinal localization, edges orientation, binocular disparity, color .. in a "interlaced" way) are represented onto cortical maps. This must be represented by a non-linear space with a variable metric, i.e. a Riemannian manifold (see e.g. [46] for an extended discussion).

In order to define this map, we consider the following optimization problem (as discussed e.g. in [12]):

$$\mathbf{h} = arg\ min \mathcal{L} \text{ with } \mathcal{L} = \frac{1}{2} \int \underbrace{||\mathbf{h} - \bar{\mathbf{h}}||^2_{\mathbf{\Lambda}}}_{\text{input}} + \underbrace{||\nabla \mathbf{h}||^2_{\mathbf{L}}}_{\text{regularization}} \quad (1)$$

where $\nabla^k_j \mathbf{h}(\mathbf{x}) = \frac{\partial \mathbf{h}^k(\mathbf{x})}{\partial x^j}$ is the $m \times n$ Jacobian matrix which corresponds to the variation of the function $\mathbf{h}$, while:

$$||\mathbf{h} - \bar{\mathbf{h}}||^2_{\mathbf{\Lambda}} = \sum_{kl} \left(\mathbf{h}^k - \bar{\mathbf{h}}^k\right)^T \mathbf{\Lambda}_{kl} \left(\mathbf{h}^l - \bar{\mathbf{h}}^l\right)$$

and

$$||\nabla \mathbf{h}||^2_{\mathbf{L}} = \sum_{ijkl} \nabla \mathbf{h}^k_i(\mathbf{x})\, \mathbf{L}^{ij}_{kl}(\mathbf{x})\, \nabla \mathbf{h}^l_j(\mathbf{x})$$

In words, the *specification* of this map of values corresponds to an "objective" or a "criterion" to attain. This criterion is built from two terms:
(i) the input term, related to the data input
(i.e. looking for a solution as compatible as possible with the input) and
(ii) the regularization term, related to the a-priori information
(i.e. looking for a solution with plausible properties: here which variation is minimal).

Regarding the term related to the input :

- $\mathbf{\Lambda} : \mathcal{R}^n \rightarrow \mathcal{R}^{m \times m} \in W^{s,\infty}(\mathcal{R}^n)$ is a, so called, *measurement information metric*, which, for the previous definition to be coherent, is :
  - symmetric i.e. $\mathbf{\Lambda} = \mathbf{\Lambda}^T$ and
  - positive i.e. so that $\forall \mathbf{v} \in \mathcal{R}^m, \mathbf{v}^T\, \mathbf{\Lambda}\, \mathbf{v} \geq 0$.

  This metric allows to represent:
  (i) the *precision of the input function*: the higher this precision in a given direction, the higher the value of $\mathbf{\Lambda}$ in this direction (in a statistical framework, $\mathbf{\Lambda}$ corresponds to the inverse of a covariance matrix)
  (ii) *partial observations*: if the input function $\bar{\mathbf{h}}(\mathbf{x})$ is only defined in some directions, it corresponds to a matrix $\mathbf{\Lambda}$ definite only in these directions (for instance, if $\bar{\mathbf{h}}(\mathbf{x})$ is only defined in the direction $\mathbf{u}$ at a given location we write $\mathbf{\Lambda} = k\, \mathbf{u}\, \mathbf{u}^T$ for some k),
  (iii) *missing data*: if the input function $\bar{\mathbf{h}}(\mathbf{x})$ is not defined for some $\mathbf{x}$, we simply have to state $\mathbf{\Lambda} = 0$ at this location; more generally it represents:
  (iv) *linear relations between some measures* $\mathbf{m}$ *and the parameter estimation* $\mathbf{h}$, say $\mathbf{M}\, \mathbf{h} = \mathbf{m}$, which is obviously equivalent to require

$||\mathbf{h} - \bar{\mathbf{h}}||^2_{\mathbf{\Lambda}} = 0$ with $\mathbf{\Lambda} = \mathbf{M}^T\,\mathbf{M}$ and $\bar{\mathbf{h}} = \mathbf{M}^T\,\mathbf{m}$ (see e.g. [68] for a development).

On the other hand, regarding the term related to "regularization":

- $\mathbf{L} : \mathcal{R}^n \rightarrow \mathcal{R}^{m\times n\times m\times n} \in W^{s,\infty}(\mathcal{R}^n)$ is a, so called, *diffusion tensor* $\mathbf{L}$, which is :
  - symmetric i.e. $\mathbf{L}^{ij}_{kl} = \mathbf{L}^{ji}_{lk}$ and
  - "positive" i.e. so that $\forall \mathbf{M} \in \mathcal{R}^{m\times n}, \mathbf{M}^T\,\mathbf{L}\,\mathbf{M} = \sum_{ijkl} \mathbf{M}^k_i\,\mathbf{L}^{ij}_{kl}\,\mathbf{M}^l_j \geq 0$
  in order the previous definition to be coherent. It defines the *profile* of this regularization.

  Thanks to the *regularization* term $||\nabla\mathbf{h}||^2_{\mathbf{L}}$, since the variation of $\mathbf{h}$ is minimized, a "smoothed" but also well-defined version of $\mathbf{h}$ is obtained [62].

  (a) When the problem is ill-posed, i.e. if there are many (and usually numerically unstable) solutions, the key idea is to choose the solution which variations are minimized: this defines a unique solution but also a well-defined solution.

  (b) When the input function is partially or approximately defined at some points, as discussed previously, the value at such a point is defined using information "around" which diffuses (as discussed now) from well-defined values to undefined or ill-defined values.

Regularization as a diffusion mechanism. A necessary condition for a function $\mathbf{h}$ to be an extremum of the criterion (1) is that the so called "normal" or Euler-Lagrange equation is verified. Here (see e.g. [66]), (1) is minimal only if:

$$\nabla_{\mathbf{h}}\mathcal{L} = \frac{\partial\mathcal{L}}{\partial\mathbf{h}} = \mathbf{\Lambda}\,\mathbf{h} - \mathbf{\Lambda}\,\bar{\mathbf{h}} - \Delta_{\mathbf{L}}\mathbf{h} = 0 \tag{2}$$

with a so-called term of diffusion:

$$[\Delta_{\mathbf{L}}\mathbf{h}]_k = \sum_{lj} \mathbf{M}^j_{kl}\,\frac{\partial\mathbf{h}^l}{\partial x^j} + \sum_{ijl} \mathbf{L}^{ij}_{kl}\,\frac{\partial^2\mathbf{h}^l}{\partial x^i\partial x^j} \tag{3}$$

with: $\mathbf{M}^j_{kl} = \sum_i \frac{\partial\mathbf{L}^{ij}_{kl}}{\partial x^i}$.

This equation simply states that, at an extremum, the criterion is locally "flat" i.e. its 1st order variation vanishes.

The term of diffusion $\Delta_{\mathbf{L}}\mathbf{h}$ allows to "propagate" some information about $\mathbf{h}$ from one point $\mathbf{x}$ to another, because it depends on the variation of $\mathbf{h}$ at $\mathbf{x}$ i.e. on what happens "around" $\mathbf{x}$.

Clearly, without the term of diffusion, the solution is $\mathbf{h} = \bar{\mathbf{h}}$.

Obviously, at the implementation level, the key problem is the calculation of $\Delta_{\mathbf{L}}\mathbf{h}$.

In order to solve (2) which corresponds to the *gradient* of the criterion (1) a 1st order *gradient descent* is usually proposed[7], starting at time $t = 0$ from the initial value $\mathbf{h}_0 = \bar{\mathbf{h}}$ and following the opposite direction of this gradient:

$$\frac{\partial \mathbf{h}_t}{\partial t} = -[\nabla_{\mathbf{h}}\mathcal{L}]_t = \left[\mathbf{\Lambda}\,\mathbf{h}_t - \mathbf{\Lambda}\,\bar{\mathbf{h}}_t - \Delta_{\mathbf{L}}\mathbf{h}_t\right] \tag{4}$$

It leads to a local minimum of the criterion, when iteratively computed using, e.g. an Euler rule of the form: $\mathbf{h}_{t+1} = \mathbf{h}_t + \Delta t\,\frac{\partial \mathbf{h}_t}{\partial t}$.

Here, since the related quadratic criterion is convex, calculating the *local* partial differential equation (4) at each point leads to the *global* minimization of the criterion (1).

Relation with linear filtering. The present mechanism is easily related to a linear filtering operator in the case where $\mathbf{\Lambda}$ and $\mathbf{L}$ are constant. In this particular case, (2) is now a linear differential equation with constant coefficients.

If we consider the Fourier transform $\mathcal{F}[\mathbf{h}(\mathbf{x})] = \mathbf{h}(\mathbf{w})$ of the quantities in (2), using the explicit form given in (3), it is straightforward to obtain in the Fourier domain:

$$\mathbf{h}(\mathbf{w}) = \mathbf{G}_{\mathbf{\Lambda},\mathbf{L}}(\mathbf{w})\,\bar{\mathbf{h}}(\mathbf{w}) \text{ with } \mathbf{G}_{\mathbf{\Lambda},\mathbf{L}}(\mathbf{w}) = [\mathbf{\Lambda}_{kl} + \sum_{ij} \mathbf{L}^{ij}_{kl}\,w_i\,w_j]^{-1}\,\mathbf{\Lambda} \tag{5}$$

[7] **About 1st order scheme convergence**. The partial differentiation rule writes $\frac{\partial \mathcal{L}}{\partial t} = \nabla_{\mathbf{h}}\mathcal{L}\,\frac{\partial \mathbf{h}}{\partial t}$. Considering $\frac{\partial \mathbf{h}}{\partial t} = -\nabla_{\mathbf{h}}\mathcal{L}$ as in (4) yields $\frac{\partial \mathcal{L}}{\partial t} = -||\nabla_{\mathbf{h}}\mathcal{L}||^2 < 0$ so that the criterion is strictly decreasing. Since $\mathcal{L} \geq 0$ it is also bounded and thus converges towards a minimal value. At this local or global minimum $||\nabla_{\mathbf{h}}\mathcal{L}|| = 0$ so that $\mathcal{L}$ is stationary. In fact, the gradient magnitude smoothly decreases with time. In practice, convergence is detected as soon as the gradient is below a given numerical threshold, which always occurs in finite time.

so that we finally obtain the convolution: $\mathbf{h}(\mathbf{x}) = \mathbf{G}_{\mathbf{\Lambda},\mathbf{L}}(\mathbf{x}) * \bar{\mathbf{h}}(\mathbf{x})$.

From (5), it is visible that the corresponding linear filter is defined by the $n^2 + m^2\, n\,(n+1)/2$ coefficients of $\mathbf{\Lambda}$ and $\mathbf{L}$ (the former being a general $n \times n$ matrix, the latter being a symmetric tensor). From obvious linear algebra in the general case, $\mathbf{G}_{\mathbf{\Lambda},\mathbf{L}}(\mathbf{w})$ is a rational fraction with a denominator of degree less than $2\,n$ and a numerator of degree less than $2\,(n-1)$. This corresponds to rather general filters, although not all linear filters can be defined from such a formula.

A step ahead, as shown in [64], if $\mathbf{L}$ is constant and if $\mathbf{\Lambda}$ is negligible, $G_{\mathbf{\Lambda},\mathbf{L}}$ corresponds, at a given time t of the diffusion process defined in (4) to an oriented Gaussian kernel:

$$G_{\mathbf{L},t}(\mathbf{x}) = \frac{1}{4\,\pi\,t}\, e^{-\frac{\mathbf{x}^T\,\mathbf{L}^{-1}\,\mathbf{x}}{4\,t}}$$

However, in both cases, defining the problem from (1) is more informative than defining a filter, since we formally define what is the "objective". Furthermore, implementing it using (4) is much more efficient than explicitly computing a convolution at each point.

A step ahead, if $\mathbf{\Lambda}$ and $\mathbf{L}$ are not constant, the present framework allows to define complex input/output relationships between $\bar{\mathbf{h}}$ and $\mathbf{h}$ which are more general than what is obtained by a linear filter, introducing some "coupling" between each local convolution. This is also called bilateral filtering [3].

From regularization to neuronal networks.

Integral form of the diffusion operators. Considering the Dirac distribution $\delta(\mathbf{x})$ (see [57] for an introduction) we may formally rewrite (3):

$$[\Delta_{\mathbf{L}}\mathbf{h}]_k = \sum_k \sigma_{kl} * \mathbf{h}^l = \int_{\mathcal{R}^n} \sum_l \sigma_{kl}(\mathbf{x}-\mathbf{y})\,\mathbf{h}^l(\mathbf{y})\,d\mathbf{y}$$

with:

$$\sigma_{kl} = \sum_j \mathbf{M}_{kl}^j\,\frac{\partial \delta^l}{\partial x^j} + \sum_{ij} \mathbf{L}_{kl}^{ij}\,\frac{\partial^2 \delta^l}{\partial x^i \partial x^j}$$

where $*$ is the convolution product. In words, there is a direct mathematical and canonical link between a differential and an integral operator.

It verifies the conservation property:

$$\int_{\mathcal{R}^n} \Delta_{\mathbf{L}}\mathbf{h}(\mathbf{x})\, d\mathbf{x} = 0 \tag{6}$$

in coherence with the physical law of conservation property for diffusion processes. In words, we want to balance the $\mathbf{h}$ values in the information diffusion process, i.e. guaranty that if we reduce the value at one location it will increase elsewhere accordingly, as in a fluid which particles are neither created nor deleted. This guarantees the stability of the numerical computations.

Furthermore, this is a "punctual" integral operator in the sense its magnitude is zero except at $\mathbf{x}$. Considering a quadratic semi-norm (i.e. its variance or inertia), it writes:

$$\int_{\mathcal{R}^n - B(\mathbf{x},\varepsilon)} \sigma_{kl}(\mathbf{x}-\mathbf{y})^2\, d\mathbf{y} = 0 \tag{7}$$

where $B(\mathbf{x},\varepsilon)$ is a ball around $\mathbf{x}$ of radius ε, which can be as small as possible, but must be excluded, in order (7) to be well-defined because the product of two distributions is not necessarily a distribution.

Optimal approximation of the diffusion operators. It is not possible in practice to implement the "punctual" operator $\Delta_{\mathbf{L}}\mathbf{h}$ because what is given, in the real world, is a set of "samples".

More precisely, we have to consider a set of "measures", defined as integral values of the continuous function over the measurement sensor receptive field. Furthermore, since numerical values contains uncertainties, it is a reasonable choice to "average" several values in order to smooth these uncertainties.

This legitimates the fact, at that the implementation level, a differential operator is approximated using an integral operator.

Based on this remark and following [50, 11, 66], we approximate the differential operator by an integral operator of the form:

$$[\Delta^*_{\mathbf{L}}\mathbf{h}(\mathbf{x})]_k = \sum_l \left[\int_{\mathcal{R}^n} \sigma^\epsilon_{kl}(\mathbf{x},\mathbf{y})\, \mathbf{h}^l(\mathbf{y})\, d\mathbf{y}\right] - \bar{\sigma}^\epsilon_{kl}(\mathbf{x})\, \mathbf{h}^l(\mathbf{x}) \tag{8}$$

with $\bar{\sigma}^\epsilon_{kl}(\mathbf{x}) = \int_{\mathcal{R}^n} \sigma^\epsilon_{kl}(\mathbf{x},\mathbf{y})\, d\mathbf{y}$

For such an approximation to be well-defined[9], the integral must be convergent. Here, to obtain this property, we assume that $\sigma^\epsilon(\mathbf{x},\mathbf{y})$ has a bounded support $\mathcal{S}$, *included in a ball* $\mathcal{B}(\mathbf{x},\epsilon)$ *of radius* $\epsilon > \varepsilon$, i.e. $\mathcal{S} \subset \mathcal{B}(\mathbf{x},\epsilon)$.

The 2nd term allows to verifies the conservation property, as soon as the kernel average is symmetric, i.e.

$$\int_{\mathcal{S}} \sigma^\epsilon_{kl}(\mathbf{x},\mathbf{y})\, d\mathbf{x} = \int_{\mathcal{S}} \sigma^\epsilon_{kl}(\mathbf{y},\mathbf{x})\, d\mathbf{x} \tag{9}$$

as derived in [66]. Such kernel are not necessarily symmetric.

It appears as an operator which *computes a weighted mean value around* $\mathbf{x}$ *minus the balanced value at* $\mathbf{x}$.

It is easy to verify that, if $\sigma^\epsilon_{kl}(\mathbf{x},\mathbf{y}) = \sigma_{kl}(\mathbf{x}-\mathbf{y})$ then $[\Delta^*_{\mathbf{L}}\mathbf{h}]_k = [\Delta_{\mathbf{L}}\mathbf{h}]_k$ and the "exact" operator $\Delta_{\mathbf{L}}\mathbf{h}$ is a particular case of the "approximate" operator $\Delta^*_{\mathbf{L}}\mathbf{h}$.

Requiring, σ^ϵ_{kl} to be around each point $\mathbf{x}$ as closed as possible to the "exact" operator σ_{kl}, we formalize this proximity by the following quadratic criterion:

$$\min_{\sigma^\epsilon} \int_{\mathcal{S}} \sigma^\epsilon_{kl}(\mathbf{x},\mathbf{y})^2 d\mathbf{x}d\mathbf{y} \tag{10}$$

In words, we use a maximal amount of information close to the point: the "sharpest" the operator, the best.

It is easily shown [66] that minimizing (10) is equivalent to choose $\sigma^\epsilon_{kl}(\mathbf{x},\mathbf{y})$ as close as possible to "exact" operator $\sigma_{kl}(\mathbf{x}-\mathbf{y})$ for a quadratic distance, related to the semi-norm specified in (7).

Relations between integral and differential operators. In order to relate the differential operator $\Delta_{\mathbf{L}}\mathbf{h}$ with its integral approximation $\Delta^*_{\mathbf{L}}\mathbf{h}$, let us identify $\Delta_{\mathbf{L}}\mathbf{h}$ with the Taylor expansion of $\Delta^*_{\mathbf{L}}\mathbf{h}$ at some order r.

Here, we consider the Taylor expansion of $\mathbf{g}(\mathbf{y},\mathbf{x}) = \mathbf{h}(\mathbf{y}) - \mathbf{h}(\mathbf{x})$ with respect to $\mathbf{y}-\mathbf{x}$.

In other words, we consider the following change of variables $\mathbf{d} = \mathbf{y}-\mathbf{x}$ and, say, $\mathbf{s} = (\mathbf{y}+\mathbf{x})/2$ in order to write the expansion with respect to $\mathbf{d}$:

[9] In addition, this operator must belong to a well-defined functional space. Here following [11] again, we consider a subset of the distributions: the Sobolev function space $W^{s,\infty}(\mathcal{R}^n)$. In fact, we are going to obtain solutions which are ordinary differentiable functions, so that it is only a formal point.

$$\mathbf{g}(\mathbf{y},\mathbf{x}) = \sum_{|\alpha|=1}^{r} \frac{\partial^\alpha \mathbf{h}}{\alpha!}(\mathbf{x})\Big|_{\mathbf{y}=\mathbf{x}} (\mathbf{y}-\mathbf{x})^\alpha + o(||\mathbf{y}-\mathbf{x}||^r)$$

and a few algebra yields:

$$[\Delta^*_{\mathbf{L}}\mathbf{h}]_k = \sum_{l=1}^{m}\sum_{|\alpha|=1}^{r} \frac{\partial^\alpha \mathbf{h}^l}{\alpha!} \int_{\mathcal{S}} \sigma^\epsilon_{kl}(\mathbf{x},\mathbf{y})\,(\mathbf{y}-\mathbf{x})^\alpha\, d\mathbf{y} + [R^r\mathbf{h}]_k$$

where $R^\epsilon_{kl}\mathbf{h}$ is the remainder of this expansion.

If we rewrite the diffusion operator with the same notations:

$$[\Delta_{\mathbf{L}}\mathbf{h}]_k = \sum_{l=1}^{m}\left[\sum_{\mathbf{e}_j} \mathbf{M}^j_{kl}\,\partial^{\mathbf{e}_j}\mathbf{h}^l + \sum_{\mathbf{e}_i+\mathbf{e}_j} \mathbf{L}^{ij}_{kl}\,\partial^{\mathbf{e}_i+\mathbf{e}_j}\mathbf{h}^l\right]$$

we easily identify the two expressions and obtain:

$$\begin{array}{lllllll}
r \geq |\alpha| > 2 & & & \int_{\mathcal{S}} \sigma^\epsilon_{kl}(\mathbf{x},\mathbf{y})\,(\mathbf{y}-\mathbf{x})^\alpha\, d\mathbf{y} & = & 0_r & [\text{C0}] \\
|\alpha| = 2 & 2\,\mathbf{L}^{ij}_{kl}(\mathbf{x}) & - & \int_{\mathcal{S}} \sigma^\epsilon_{kl}(\mathbf{x},\mathbf{y})\,(\mathbf{y}-\mathbf{x})^{\mathbf{e}_i+\mathbf{e}_j}\, d\mathbf{y} & = & 0_r & [\text{C2}] \\
|\alpha| = 1 & \mathbf{M}^j_{kl}(\mathbf{x}) & - & \int_{\mathcal{S}} \sigma^\epsilon_{kl}(\mathbf{x},\mathbf{y})\,(\mathbf{y}-\mathbf{x})^{\mathbf{e}_j}\, d\mathbf{y} & = & 0_r & [\text{C1}]
\end{array}$$

where $0_r = \int_{\mathcal{S}} o(\mathbf{y}-\mathbf{x})^r d\,\mathbf{y}$ is a negligible quantity for sufficiently small ϵ.

These conditions [C0] [C2] and [C1] allow to identify up to the rth order the two expressions.

Since[11] from a few algebra:

$$|\textstyle\int_{\mathcal{S}} \sigma^\epsilon_{kl}(\mathbf{x},\mathbf{y})\,(\mathbf{y}-\mathbf{x})^\alpha\, d\mathbf{y}| \leq [||\sigma^\epsilon_{kl}||_{0,\infty}\,\textstyle\int_{B(0,1)}]\,\epsilon^{|\alpha|+1}/(|\alpha|+1)$$

thus exponentially decreases with $|\alpha|$, for higher values of $|\alpha|$ the condition [C0] is numerically verified as corresponding to a negligible quantity. It is thus reasonable choice to bound $|\alpha|$ with a fixed value r.

These conditions have the interesting property to be "decoupled" in the sense that they allow, for a given (k,l) to relate each σ^ϵ_{kl} to the corresponding $\mathbf{M}_{kl}$ and $\mathbf{L}_{kl}$ independently.

Furthermore, we have a bound[3] on the error for our approximation, as a function of ϵ^{r-1} i.e.:

$$||\Delta_{\mathbf{L}}\mathbf{h} - \Delta^*_{\mathbf{L}}\mathbf{h}||_{0,\infty} = ||R^r\mathbf{h}||_{0,\infty} \leq C\,\epsilon^{r-1}||\mathbf{h}||_{r+1,\infty}$$

for a fixed constant C, since $\mathcal{S} \subset B(\mathbf{x},\epsilon)$. This, for a covering of the parameter space by supports $\mathcal{S} \subset B(\mathbf{x},\epsilon)$ organized in some mesh, allows to conclude that $\lim_{\epsilon\to 0}\Delta^*_{\mathbf{L}}\mathbf{h} = \Delta_{\mathbf{L}}\mathbf{h}$ and $\lim_{r\to\infty}\Delta^*_{\mathbf{L}}\mathbf{h} = \Delta_{\mathbf{L}}\mathbf{h}$ for small ϵ: in words, this approximation is consistent, with respect to the sampling and the Taylor expansion.

[11] Here $\int_{B(0,1)} = \frac{\pi^{n/2}}{\Gamma(n/2+1)}$ is the volume of the unit ball.

Integral approximation of a diffusion operator as a NN. In [66] with a formulation similar to the present one, the integral approximation kernel has been defined using rational functions, i.e. ratio of polynomials, yielding the possibility to defined "poles" but with the risk of numerical instabilities. We consider that, in terms of biological plausibility[12], we must define such approximation without "divisions", avoiding the risk of considering huge values whereas neuronal information has a limited range and using an operation which is not a direct biologically plausible operation.

In fact, we simply assume that a neuron code a value at a given point $\mathbf{p}_u$ of the cortical map. Values at other points are set to zero, yielding:

$$\sigma^{\epsilon}_{kl}(\mathbf{x},\mathbf{y}) = \textstyle\sum_{uv} \sigma^{uv}_{kl}\delta(\mathbf{x}-\mathbf{p}_u,\mathbf{y}-\mathbf{p}_v)$$

where $\mathbf{p}_u$ are the neuron localization in the NN map, while $\delta(\mathbf{x},\mathbf{y})$ is the vectorial $2\,n$ Dirac distribution. This sampling model, related to a so called "particle process" [11], assumes that each unit computes a discrete set of map values. It is often used in the absence of a-priori geometric knowledge on the unit distribution, which is the case for neuronal units. In comparison, in [66], for camera images processing, the sampling model of the continuous equation is based onto a simple but different model, where each unit represents an "average value" around its location which corresponds to the pixelic image formation. A perspective of this work is to consider such alternatives.

Here, equation (4), is now of the form:

$$\frac{\partial \mathbf{h}^k_t}{\partial t}(\mathbf{p}_u) = -\sum_l \left[\mathbf{\Lambda}^k_l \left[\mathbf{h}^l_t - \bar{\mathbf{h}}^l_t\right](\mathbf{p}_u) - \sum_v \sigma^{uv}_{kl}\mathbf{h}^l_t(\mathbf{p}_v)\right] \tag{11}$$

and using a, say, Euler iterative scheme of the form $\mathbf{h}_{t+1}(\mathbf{p}_u) = \mathbf{h}_t(\mathbf{p}_u) + \Delta t\,\frac{\partial \mathbf{h}_t}{\partial t}(\mathbf{p}_u)$ for sufficiently small Δt allows the convergence of this 1st order minimization algorithm towards the criterion minimum.

The implementation of (11) has the same architecture and is not more complex than any other neuronal networks NN, including Hopfield[14]networks.

[12]See e.g. [6] for details about the biological plausibility of linear and multiplicative computational steps, including motion detection and short-term memory, while [70] focuses on the biologically plausible implementation of non-linear operation such as minimum computation or comparisons between inputs.

[14] **About Hopfield networks.** Formally, a neuronal network à-la Hopfield is a discrete dynamical system defined on a set of N binary signals $\mathbf{s} = (\cdots s_u, \cdots)$ with $s_u \in \{-1, 1\}$.

Signals update is defined by a recurrent equation of the form:

$$s_u^{t+1} = Sg\left(\sum_{v=1}^{N} \sigma_{uv}\, s_v^t - \theta_u\right)$$

In some architectures this binary "activation" function is replaced by a sigmoid like profile. This is one of the oldest neuronal-network [32].
In order to update s_u^{t+1} from s_u^t one of these two rules is usually used, either:
- *parallel* update, where all signals s_u^t are simultaneously updated, or
– *random* update, where *one* signal (randomly selected) is sequentially updated at each time.
In *Hopfield* networks $\sigma_{uv} = \sigma_{vu}$ and $\sigma_{uu} \geq 0$, while random update is used. As a consequence, we can relate this dynamical system to a bounded "energy" (a.k.o. Liapounov function):

$$E = -\tfrac{1}{2} \textstyle\sum_u (\sum_v \sigma_{uv}\, s_v^t - 2\,\theta_u)\, s_u^t$$

so that when a signal s_u^t is updated we easily verify (e.g. [69]) that $\delta E < 0$. Since this bounded energy decreases with time, it must converge to a stationary value, corresponding to a stable equilibrium point.
Such a dynamical system has thus only equilibrium points as attractors. Obviously, they are characterized by the fact that $\mathbf{s}$ is not to be updated, if and only if $\forall u, s_u\, (\sum_v \sigma_{uv}\, s_v - \theta_u) \geq 0$.
In our case, with $s_u = h(\mathbf{p}_u)$ and $\theta_u(s) = \mathbf{\Lambda}\, \left[\mathbf{h} - \bar{\mathbf{h}}\right]\, (\mathbf{p}_u)$, the recurrent equation is of the same form although the signal is not binary (thus without sigmoid profile), but a vectorial value, while the threshold θ_u varies the signal.
In both cases, the NN convergence is related to a criterion minimization.
Learning in Hopfield networks. Let us consider R "prototypes" $\mathbf{s}^r, r = 1..R$ of binary signals and an Hopfield network, defined with $\sigma_{uu} = 0$, $\theta_u = 0$ and $\sigma_{uv} = \sum_{r=1}^{R} s_u^r\, s_v^r$.
The condition for a prototype $\mathbf{s}^{r_0}$ to be an attractor of this network yields:

$$s_u^{r_0} \textstyle\sum_v \sigma_{uv}\, s_v^{r_0} = N - 1 + \sum_{r \neq r_0} s_u^r\, s_u^{r_0} \sum_v s_v^r\, s_v^{r_0} \geq 0$$

which occurs if the prototypes are uncorrelated (thus linearly independent), i.e. $\sum_v s_v^r\, s_v^{r_0} \simeq 0$.
This means that for an input pattern s initializing the network, it will converges towards one attractor of index r, the index depending in which basin of attraction s is. This allows to "label" any pattern s depending on its "proximity" to an attractor, for this network. As such, its acts as a classificator.
More precisely considering the probability for a sum of binary numbers $s_u \in \{-1, 1\}$ to be below a given threshold τ, $p(\sum_{i=1}^{q} s_u < \tau) = Q(\frac{\tau}{\sqrt{q}})$ with $Q(u) = \frac{1}{\sqrt{2\,\pi}} \int_{-\infty}^{x} e^{-\frac{1}{2}u^2}$ it is shown (e.g. [69]) that we may store about $R = o(\frac{N}{2\log(N)})$ prototypes in a network of size N with a reasonable probability ($typicallyP > 0.99$) of success. Otherwise the network has a catastrophic behavior and converges towards anything.
The learning rule may also be written in an incremental form $\sigma_{uv} = \alpha\, \sigma_{uv} + \beta\, s_u^r\, s_v^r$. If $\alpha = \beta = 1$ it is equivalent to the previous form. If $0 < \alpha < 1$ and $\alpha + \beta = 1$ the pattern memorization is realized with some decay: older pattern being less taken into account. This

Contrary to this basic model, which assumes the symmetry of the weights ($\sigma^{uv} = \sigma^{vu}$) and the absence of reflexivity ($\sigma^{uu} = 0$) we have introduced here weaker assumptions: average symmetry ($\sum_u \sigma^{uv} = \sum_v \sigma^{vu}$) and conservation property, but the real difference is that these assumptions are by construction, always verified and do not introduce additional constraints.

The implementation proposed in (11) allows to consider this computation as a biological plausible mechanism. See e.g. [6] for details about the biological plausibility of linear and multiplicative computational steps.

At a higher scale, in the cortex, the "neuronal unit" is a cortical hypercolumn. Our model is thus to be mapped onto usual computational model of cortical columns processes (see [9] for a treatise on the subject), as already proposed by [36]. Such a "processing unit" [33] is discussed in e.g. [46]. Such cortical column architecture is represented in Fig. 2.

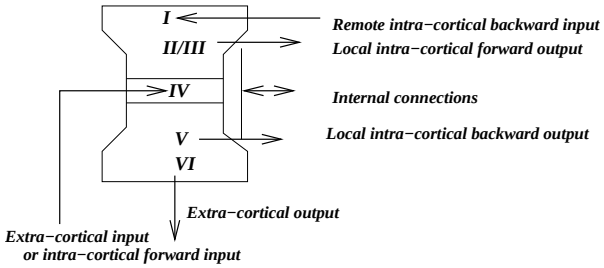

Figure 2: Schematic description of a cortical column, from [9].

so-called *palimpestre* mechanism allows to bound the network contents which helps to avoid overflow.

Another so-called "anti"-Hebbian learning rule of the form $\sigma_{uv} = \sigma_{uv} - \beta\, s_u^r\, s_v^r$ for small positive β may be used. This indeed is not used to directly memorize a given pattern but to *de-correlate* this pattern in the network. It is also used for error-correcting mechanisms [14].

Beside any biological plausibility, this classifier is a simple linear classifier based on binary prototypes to define its calibration. Such neuronal dynamics computes a comprehensive (but not easy to analyze) form of distance-to-prototype computation.

In the *perceptron* mechanism (e.g. [59] for a didactic introduction), such a neural network is used to design linear classifiers, with a training based on a gradient minimization algorithm.

We propose to consider the link between the neuronal computation architecture and the structure of a cortical columns as follows:
- *extra cortical input or intra-cortical input from previous layers* (layers IV of the cortex) correspond to the input variable $\bar{\mathbf{h}}$,
- *extra cortical or backward intra-cortical output* (layers V of the cortex) correspond to the output the computed variable $\mathbf{h}$,
- *local intra cortical connections* (layers II/III of the cortex) correspond to inter-parameters interaction, i.e. forward inputs to define $\mathbf{\Lambda}$ and $\mathbf{L}$, thus σ,
- *backward intra cortical connections* (layers I of the cortex) correspond to inter-parameter interactions, i.e. backward inputs to define $\mathbf{\Lambda}$ and $\mathbf{L}$, thus σ,
- *internal connections* correspond to the local diffusion mechanism, i.e. correspond to the integration over the operator variable.

Learning the NN weights in this framework. Given a cortical map computation unit, as proposed in (11), parameterized by $\mathbf{\Lambda}$ and $\mathbf{L}$ thus $\mathbf{M} = div(\mathbf{L})$, the next step is to describe how to derive σ. In other words, we have to explain how to proceed to "what is to be done" as stated in (1) to "how to do it" as stated in (11).

Minimizing the quadratic criterion (10) with the linear constraints [C0] [C2] [C1] and (9) yields the following convex quadratic problem, for a given kl, with a unique generic solution obvious to derive:

$$\min \sum_{uv} (\sigma_{kl}^{uv})^2 \text{ with } \begin{array}{l} \forall u, \sum_v \sigma_{kl}^{uv} (\mathbf{p}_u - \mathbf{p}_v)^\alpha = \left\{ \begin{array}{rrcl} 0 & |\alpha| & > & 2 \\ 2\,\mathbf{L}_{kl}^{ij}(\mathbf{p}_u) & \alpha & = & \mathbf{e}_i + \mathbf{e}_j \\ \mathbf{M}_{kl}^{j}(\mathbf{p}_u) & \alpha & = & \mathbf{e}_j \end{array} \right. \\ \sum_v \sigma_{kl}^{uv} = \sum_u \sigma_{kl}^{uv} \end{array} \tag{12}$$

For a given kl, writing $w = (u, v)$ and σ_{kl}^{w} the vector indexed by w, (12) writes:

$$\min_\sigma ||\sigma||^2 \text{ with } \mathbf{C}\,\sigma = \mathbf{b}$$

where $\mathbf{b} = (0 \cdots 2\,\mathbf{L}_{kl}^{ij}(\mathbf{p}_u) \cdots \mathbf{M}_{kl}^{j}(\mathbf{p}_u) \cdots)$ is the problem input, while the coefficients of the matrix $\mathbf{C}$ are constant and either of the form $(\mathbf{p}_u - \mathbf{p}_v)^\alpha$ or in $\{-1, 0, 1\}$ as directly derived from (12). This matrix $\mathbf{C}$ only depends on the map geometry, neither on its input nor on its values.

This compact form allows to write, in the general case, the explicit solution: $\bar{\sigma} = \mathbf{C}^T (\mathbf{C}\,\mathbf{C}^T)^{-1}\,\mathbf{b}$ with $||\bar{\sigma}||^2 = ||\mathbf{b}||^2_{(\mathbf{C}\,\mathbf{C}^T)^{-1}}$ (see [68] for a derivation and a complete discussion). The key pointis that this solution is easily calculable using an iterative learning rule of the form:

$$\sigma_{t+1} = \sigma_t - \gamma$$

which converges[17] as soon as γ verifies $\gamma^T\,\mathbf{g} > \frac{1}{2}\,||\gamma||^2_{\mathbf{C}^T\,\mathbf{C}}$ with $\mathbf{g} = (\mathbf{C}^T\,\mathbf{C})\,\sigma_t - \mathbf{C}^T\,\mathbf{b}$, i.e. as soon as $||\gamma||$ is small enough and γ in the direction of $\mathbf{g}$ (i.e. $\gamma^T\,\mathbf{g} > 0$). When $\mathbf{g} = 0$ we obtain $\sigma = \bar{\sigma}$ and the iteration stops. The vector $\mathbf{g}$ is easily computed as a linear combination of the input $\mathbf{b}$ and the estimate σ and the end of the iteration easily detected when $\mathbf{g} = 0$.

Since this learning rule is still valid for approximate values of γ, biological networks can thus easily implement this rule. This kind of linear learning rule is a particular case of Hebbian learning rule (see [14, 49] for an experimental discussion and [19] for a theoretical development).

What is interesting here, is that the present formalism is related to a tuning mechanism simple enough to be mapped on existing model of biological neuronal networks. More precisely, this derivation is in coherence with [70] who focus on the biologically plausible implementation of non-linear operation such as minimum computation or comparisons between inputs.

However, at this level of description, how the cortical map parameters are learned is an open question, not addressed here.

[17] This fact is obvious, considering the minimization of $\frac{1}{2}\,||\sigma - \bar{\sigma}||^2_{\mathbf{C}^T\,\mathbf{C}}$ with:

$$\frac{1}{2}\,||\sigma_{t+1} - \bar{\sigma}||^2_{\mathbf{C}^T\,\mathbf{C}} = \frac{1}{2}\,||\sigma_t - \bar{\sigma}||^2_{\mathbf{C}^T\,\mathbf{C}} - \gamma^T\,\mathbf{g} + \frac{1}{2}\,||\gamma||^2_{\mathbf{C}^T\,\mathbf{C}}$$

this convex quadratic criterion being minimum iff $\sigma = \bar{\sigma}$. From the previous equation, $\frac{1}{2}\,||\sigma_{t+1} - \bar{\sigma}||^2_{\mathbf{C}^T\,\mathbf{C}} < \frac{1}{2}\,||\sigma_t - \bar{\sigma}||^2_{\mathbf{C}^T\,\mathbf{C}}$ iff $\gamma^T\,\mathbf{g} > \frac{1}{2}\,||\gamma||^2_{\mathbf{C}^T\,\mathbf{C}}$ so that this bounded criterion decreases as soon as the condition is verified.
The condition $\gamma^T\,\mathbf{g} > \frac{1}{2}\,||\gamma||^2_{\mathbf{C}^T\,\mathbf{C}}$ implies that $\gamma^T\,\mathbf{g} > 0$, i.e. that γ and $\mathbf{g}$ are in the same direction (but not necessary aligned). A step further, let us write $\mathbf{u} = \gamma/||\gamma||$. For a fixed $\mathbf{u}$, as soon as $||\gamma|| < 2\,\mathbf{u}^T\,\mathbf{g}/||\mathbf{u}||^2_{\mathbf{C}^T\,\mathbf{C}}$ the condition is verified. Therefore, as soon as $||\gamma||$ is small enough and $\gamma^T\,\mathbf{g} > 0$ the convergence is obtained.
Finally the gradient of this quadratic criterion is precisely equal to $\mathbf{g}$: as a consequence $\mathbf{g} = 0 \Leftrightarrow \sigma = \bar{\sigma}$.

Examples of cortical maps computations in the visual cortex.

The visual cortical areas of the primate (see e.g. [65] for a comparative description of the organization of visual areas in macaque and human cerebral cortex) has two main streams: the ventral[18] and dorsal[19] considered as the "what" (i.e. object recognition) and "where" (i.e. object localization and motion analysis) processing streams, respectively.

Linking network equations and regularization mechanisms. Neural networks models are based upon network equations of what is called "cell activity", basic network equations are identical to neuronal membrane potential equations [31] of the form:

$$-C\frac{\partial V}{\partial t} = \sum_u g_u(V - V_u)$$

where C is the membrane capacitance and g_u are different conductances related to different cell's properties (synaptic excitatory or inhibitory conductance, ionic channels, leaking current, shunting inhibition, ..). A steady-state behavior is often considered i.e. when $\frac{\partial V}{\partial t} = 0$. The relation with our framework is obvious: the components of the cortical map vector $\mathbf{h}$ at one point is precisely the cell activity parameters. Since the parameter $\mathbf{h}$ is not a unique value but a vector it is possible to consider several quantitative indicators of the neuronal activity.

[18]**The "ventral" pathway:** Prior to the inferior temporal cortical area, is the so called parietal/ventral pathway (sometimes improperly called "parvocellular" pathway), neurons in the inter-blobs of V1 project to the pale stripes of V2. This pale stripes of V2 project to the inferior temporal cortex. Other feed-forward pathways include the V4 visual area, see [8] for general review. This pathway is composed of feature detectors (simple, complex and hyper-complex cells) (e.g. [33] for an introduction). Neurons in this pathway show a low sensitivity to contrast, high spatial resolution, and low temporal resolution or sustained responses to visual stimuli. See for instance [14], Chap 2 for a discussion.

[19]**The "dorsal" pathway:** Here a second visual cortical pathway, parietal an dorsal, in which the neurons in layer 4B of V1 project to the thick stripes of V2 is considered. Area V2 then projects to V3, V5 (or MT, middle-temporal cortex), and MST (median superior temporal cortex) This pathway is mainly an extension of the magnocellular pathway, but not only.

A step ahead, such models assume that some cortical maps also perfom linear filtering operations: e.g. Gaussian or Gabor linear filtering. As reviewed previously, there is a direct implementation of Gaussian oriented filters as regularization mechanisms, while Gabor filters may easily be approximated in this framework also (see e.g. [28] for a discussion about inverse heat equation).

Considering the models introduced, for instance by Grossberg and collaborators, a crucial property is that these models are only based on membrane equations and linear filtering operations, plus two other ingredients:
- interaction (feed-forward but also backward) between such cortical map computations,
- rectification (eventually with a threshold θ) to take into account the fact that "neuronal activity values" (spiking rate but also 1st spike delay, etc..) are positive numbers. Authors usually consider $u \rightarrow [u-\theta]^+ = max(u-\theta, 0)$, the output of one level being rectified before fed into the next level. In [58] a variant is proposed, using half-square rectification: $u \rightarrow ([u-\theta]^+)^2$.

Both aspects: interaction and rectification are going to be discussed in the next section.

The idea of introducing regularization mechanisms to represent cortical map computations is not entirely new: at a cognitive level, considering interpolation between prototypes of gestures, [21] attempts to interpret how the cortical "what" and "where" pathways of the visual cortex are involved in complex movements patterns. For instance, a complex spatio-temporal pattern is efficiently represented as a combination of prototypes whose coefficients are estimated using variational estimation methods [20].

Using network equations to simulate the brain behavior. Several aspects of visual perception are simulated using such networks equations, including cognitive mechanisms such as perceptual grouping. For instance, [26] attempts to demonstrate how the known laminar architecture of the V1 and V2 areas of the visual cortex, assuming a functional role for this stratification, is involved in percepts generation, see also [43]. This includes pre-attentive/attentive aspects, as pointed out by [47] describing how the parvocellular stream of the visual cortex performs visual filtering, i.e. attention and perceptual grouping, using feed-forward, feedback and horizontal interactions. For instance, figure / ground segmentation in the brain, as recently reviewed

by [52] showing that shape perception depends critically on this cue, while its link to early-vision mechanisms is now relatively well understood [53] e.g. the role of junctions in surface completion and contour matching.

Considering the ventral stream, the work of [41] is a recent attempt to explain how complex cells can issue depth percepts for binocular but also monocular (i.e. da Vince stereopsis) cues, including induced effects from contrast changes (i.e. shape from illumination) as simulated in [25]. This also includes disparity tuning: [27] develops a model explaining how the LGN is involved in binocular disparity tuning, matching left and right images with the same contrast polarity but inducing feedback adaptation from signals of opposite polarities.

Considering the other stream, motion processing[21] is a key problem. The visual motion of rigid objects can be analyzed through two stages, one that responds to the oriented image components, and one that finds the motion consistent with these components. A physiologically plausible model for both type of MT cells has been proposed [4, 58]. In these models, MT cells combine the output of appropriate model V1 cells. These models account qualitatively for a wide range of phenomena [40]. Stability of such cortical map comutations is obtained using a global normalization, related -according to the authors- to control of the overall conductance of the cell's membrane. Such assumption

[21] **About motion processing.** Here, we have in mind the dorsal cortical visual pathway, sometimes called magnocellular visual pathway extension, in which the neurons in layer 4B of V1 project to the thick stripes of V2 is considered. Area V2 then projects to V3, V5 (or MT, middle-temporal cortex), and MST (medial superior temporal cortex). This pathway is an extension of the magnocellular pathway from the retina and LGN, and continues the processing of visual detail leading to the perception of shape in area V3 and movement in areas V5 and MST. See [8] for a discussion.
As far as motion perception is concerned, simplifying the situation: cells in V5 are particularly sensitive to small moving objects or the moving edge of large objects; cells in dorsal MST respond to the movement of large scenes such as is caused with head movements; cells in ventral MST respond to the movement of small objects against their background. See for instance [14], Chap 10 for a discussion.
Such magnocellular neurons, deeply related to motion perception, show a high sensitivity to contrast, low spatial resolution, and high temporal resolution or fast transient responses to visual stimuli. These cellular characteristics make the magnocellular division of the visual system especially able to quickly detect novel or moving stimuli.

about "global normalization" is not required in our framework, since stability is related to the conservation property which is implemented by a local process.

How the PDE approach may help in this context. The theoretical limitation of the previous approaches is the fact that for each model instance, "ad hoc" non-trivial mechanisms must be designed in order to guaranty the stability of the whole system and finally only a (necessarily limited) set of simulations demonstrates the model's plausibility for a short range of stimulus. On the contrary, here, we propose a well-known but useful framework in which the convergence within any cortical map computation is guarantied. Interactions between cortical map computations (as discussed in the sequel) will also appears as intrinsically well-defined and stable.

Furthermore, as discussed in [66], there is a direct link between such a biological architecture and efficient regularization based algorithms of motion estimation in computer vision developed. For instance (e.g. [42]) edge orientation is a basic cue to regularize motion computation: motion computation is propagated in contrast-less areas and along edges but not across edges. This allows to obtain well-defined motion maps, preserving boundaries.

Finally, motion is at this stage, not simply parameterized by the local velocity field. Well-known early vision visual cues (e.g. the Koenderinck *def* value easily computed by an affine modelization of the retinal motion field [10]) are relevant candidates for such a parameterization. The present framework can very simply allows to take different parameters into account, as discussed now for one example.

The kinematic boundaries computation example. Yet another further, another example of motion perception, kinetically defined boundaries, extensively studied in V1/V2 [38] and in MT [39] but also in the KO region [45] and IT [56], may be easily explained within in this architecture.

> Kinetic boundaries separate two regions of motion with the same structure (e.g. random moving dots) but with different motions (e.g. motion in different directions). Usual analyses of the processing in areas V1/V2, V3 and V5 during the perception of coherent and incoherent motion [35] or more sophisticated motion

detector models such as those related second order motion [34] does not explain this perception [38, 56].

- More precisely, selectivity for the orientation of the motion-defined boundaries first emerges in area V2 where neurons are selective for the orientation of kinetic edge stimuli (contrary to neurons in V1 [38]), also displaying a strong sharply tuned response to a luminance edge of the same orientation. Responses for the motion-defined boundaries orientation are about 40ms more slowly than for luminance edges, suggesting a feedback entering the ventral stream at a point downstream with respect to V2.
- A step ahead, in area MT, cells are more selective to the local direction of motion than to luminance orientation, but with a preferred direction aligned with their preferred direction. These cells appear to respond to the average motion vector over their receptive field, but are unable to code the orientation of the kinetic boundaries [39]. This directionality remains unaltered by the presence of additional motion vectors, so that MT cells extract only motion in a specific direction.
- The cortical region specialized for the processing of kinetic boundaries is the so-called Kinetic Occipital (KO) region in man [45], distinct from MT/V5, V3 and V3A. This region is activated by kinetic gratings with discontinuities in motion direction much more than luminance defined, uniform motion or transparent motion gratings. This activation is relatively independent from stimulus size, spatial frequency or to the kind of generated kinetic boundary.
- Finally, cells in the IT area respond well to several gratings, independently of the cue used to defined this gratings: static (luminance, texture) or kinetic boundaries. The latencies for static gratings are significantly shorter than for kinetic ones. Only a small proportion of cells are sensitive for more than one cue, but in this case the averaged preferred orientation matches. This suggests that IT cells may contribute to cue-

invariant coding of boundaries and edges, although kinetic boundaries requires more iterations in the upstream.

These facts allow us to discuss how kinematic boundaries computation may occur considering interactions between cortical maps. Our key idea is that *as soon as a (here vectorial) motion map is computed in MT, kinematic boundaries are simple (vectorial) edges of the local motion map*. On one hand, an area like KO can easily inputs from MT a motion map input and computes edges as V1 does for luminance map: this is a simple V1$\rightarrow$MT$\rightarrow$KO$\cdots\rightarrow$IT feed-forward stream. On the other hand, the V2 area can easily process edges not with luminance as input, but using backward information from MT: in that case a V1$\rightarrow$MT$\rightarrow$V2$\cdots\rightarrow$IT feed-forward stream is assumed. It must be note that this second stream creates a "loop" in the dorsal V1$\rightarrow$V2$\cdots\rightarrow$MT$\cdots$ dorsal stream. As such, this is a source of instability. The 1st solution is thus more relevant, although it implies the implication of another area downstream to MT: precisely the KO, as discovered by neuro-scientists.

As a consequence, kinematic boundaries information is likely re-introduced in V2 in order to be combined with other cues in order to allow higher-layers such as IT to fuse different cues into a compatible percept. This is compatible with the observed delays, and as detailled by the authors, with the anatomical connections.

The fact a *specific* cortical area (hence KO) is involved in such a specific computation, does not means it is not involved in other computations. On the contrary, our framewrok postulates that each cortical area computation is entirely determined by its input $\bar{\mathbf{h}}$ and the paramaters ($\mathbf{\Lambda}$ and $\mathbf{L}$). Modifying the input taken into account or adjusting the parameters driven by other cortical maps inputs allows to "reuse" the map for another purpose. This difference between "specialization" and "segregation" is extensively discussed in [18] and is coherent with the present framework.

More generally, the next key issue is to understand how these cortical maps interact. Let us address this point now.

3 Introducing feedbacks in regularization mechanisms.

Following [18], let us recall that the cortex is to be considered as a hierarchy of cortical levels with reciprocal extrinsic cortico-cortical connections among the constituent cortical areas [17]. The notion of a hierarchy depends upon a distinction between forward and backward extrinsic connections. This distinction rests upon different laminar specificity [51, 54].

In this context, *forward connections are driving and backward connections are modulatory*, as suggested by reversible inactivation [55, 22] and functional neuro-imaging [5]. In some paradigms, backwards connections may also being functionally driving the signal if their latencies are shorter than forward connections between distant cortical maps [60]. This fact is compatible with the present formalism.

More precisely, *forward* connections are concerned with the promulgation and segregation of sensory information, consistent with: (i) their sparse axonal bifurcation; (ii) patchy axonal terminations; and (iii) topographic projections. On the other hand, *backward* connections are considered to have a role in mediating contextual effects and in the co-ordination of processing channels, consistent with: (i) their frequent bifurcation; (ii) diffuse axonal terminations; and (iii) non-topographic projections [54] (iv) slow time-constants.
Backward connections are more numerous and transcend more levels, e.g. the ratio of forward efferent connections to backward afferents in the lateral geniculate is about 1:10/20. Another example: there are backward connections from TE and TEO to V1 but no monosynaptic connections from V1 to TE or TEO [54]. Backward connections are more divergent than forward connections [71], one point in a given cortical area will connect to a region 5-8mm in diameter in another. For instance: the divergence region of a point in V5 (i.e. the region receiving backward afferents from V5) may include thick and inter-stripes in V2, whereas its convergence region (i.e. the region providing forward afferents to V5) is limited to the thick stripes [71]. They are faster than direct lateral connections [44]. As a consequence, forward connections preserve retinotopy in visual areas, whereas backward connections do not [8].

This is summarized by [18] as reported in table 1.

Forwards connections	*Backwards connections*
Sparse axonal bifurcations	Abundant axonal bifurcation
Topographically organized	Diffuse topography
Originate in supragranular layers	Originate in bilaminar/infragranular layers
Terminate largely in layer VI	Terminate predominantly in supragranular layers
Postsynaptic effects through fast	Modulatory afferents activate slow
AMPA (1.3-2.4 ms decay) and	(50 ms decay) voltage-sensitive NMDA receptors
GABAA (6 ms decay) receptors	

Table 1: Forwards/Backwards connections connections main properties, from [18].

Following [8], we must emphasize the fact that cortical visual processing requires information to be exchanged between neurons coding for distant regions in the visual field. Feedback connections from upper-layers are best candidates for such interactions because magnocellular[24] layers of the LGN[25] very rapidly project a "first-pass" information used to guide further processing in IT[26]. A

[24]**About (magno/parvo)cellular streams:** There are two classes of cells from the retina and LGN: magnocellular, and parvocellular. These two cell types are contained in different parts of the LGN, and they have different response properties: (i) magnocellular cell receptive fields are 2-3 times larger than parvocellular cell receptive, fields parvocellular have better acuity, resolution magnocellular have better sensitivity, magnocellular cells respond well to moving stimuli, whereas parvocellular cells do not parvocellular cells respond well to color stimuli, whereas magnocellular cells do not.
The magnocellular pathway (phylogenetically older than the parvocellular one) continues the processing of visual detail leading to the perception of shape in area V3 and movement in areas V5 and MST. It has less synaptic relays than the parvocellular pathway, but is faster.

[25]**About LGN:**The Lateral Geniculate Nucleus (LGN) is the neuronal relay from the retina to the cortical visual input, this structure is organized in a laminar architecture with a binocular representation.

[26]**About IT:** The inferior temporal cortex is though to consist of three parts: The TEO (the occipital division of the intra-temporal cortex), the TE (the median division), and the STS (superior temporal sulcus).The TEO is used for making discriminations between 2-D patterns which differ in form, color, size, orientation, or brightness. The TE is used for recognition of 3-D objects. Both the TE and STS are thought to be used in facial recognition and in the recognition of familiar objects. The STS may be the place in which the feature

step further, [2] demonstrate that the so called "horizontal connections" (i.e. within a cortical, e.g. retinotopic, map) are not fast enough to account for such a transfer, considering the known timings of information transfer [44].

More generally [18], feedback connections are essential when the relationship between retinal inputs and the stimuli that generate them is not invertible. This is the case for practically all situations of vision outside the laboratory because of the interactions between the stimuli and the importance of the context for a given stimulus [18]. In the Rao and Ballard [48], the way by which internal representations and incoming signals are combined is mainly subtractive : only differences are transmitted to higher levels. However, all studies of feedback connections so far [8] converge to conclude that feedback influences act to potentiate the responses of neurons at lower levels. In our framework, this occurs by tuning the cortical map parameters, formalized now.

The question here is to analyze such interactions when considering regularization mechanisms, i.e. study how our model may be used considering several cortical maps in interaction.

Formalizing the interaction between different cortical maps

Let us now consider, from (1), the definition of several cortical maps, indexed by i, i.e.:

$$\mathbf{h}_i = arg\,min\ \mathcal{L}_i \text{ with } \mathcal{L}_i = \frac{1}{2}\int ||\mathbf{h}_i - \bar{\mathbf{h}}_i||^2_{\mathbf{\Lambda}_i(\mathcal{S}*\rho(\mathbf{h}_{\bullet i}))} + ||\nabla \mathbf{h}_i||^2_{\mathbf{L}_i(\mathcal{S}*\rho(\mathbf{h}_{\bullet i}))}$$

writing $\mathbf{h}_\bullet = (\cdots \mathbf{h}_i, \cdots)$ all cortical maps values and $\mathbf{h}_{\bullet i}$ a sub-vector of $\mathbf{h}_\bullet$ which does not contains $\mathbf{h}_i$. This vector corresponds to the *backward* connections onto the map of index i. A spatial smoothing operator $\mathcal{S}$ has been introduced, to take into account the fact that backward connections are divergent, as discussed previously.

A rectification function $\rho()$ has also been introduced, e.g. $\rho(u) = max(u, 0)$ to take into account the fact that only positive quantities is output by cortical maps, as discussed previously. More generally, authors consider profiles of the form $\rho(u) = \gamma(Y(u)u)$, where $Y(u) =$ if $u > 0$ then u else 0 is the Heaviside

maps of objects (which contain separate information about each primitive of an object, such as color, orientation, or form) become object files.

function and $\gamma()$ a strictly increasing positive function in $\mathcal{R}^+$ with $\gamma(0) = \gamma'(0) = 0$ (e.g. $\gamma(u) = u^\alpha$ for some $\alpha > 1$, [58]), so that $\rho'(u) = \gamma'(Y(u)u)$, as the reader can easily verify. At this level, there is no need to further specify $\rho()$.

Here, each cortical map value can tune the other map computations, modifying the parameters $\mathbf{\Lambda}_i$ and $\mathbf{L}_i$, as made explicit in the previous equation. The key point is that such interactions are constrained:
(i) cortical value are "averaged", i.e. smoothed in space, before influencing the cortical map parameters,
(ii) a cortical map value does not modify its own parameters,
(iii) a feed-forward connection from a cortical map of index i to a cortical map of index j corresponds to the fact that $\bar{\mathbf{h}}_j = \rho(\mathbf{h}_i)$ and define a lattice (no loops between forward connections).
These constraints correspond to what has been observed in the cortex, as reviewed previously. They are fundamental in the following development.

Forward connections define a lattice of cortical maps and we can say a map of index i_l is "after another" map of index i_1, say $i_l \succ i_1$, iff $\bar{\mathbf{h}}_{i_{j+1}} = \rho(\mathbf{h}_{i_j})$ for a sequence of indexes $i_1..i_l$, defining a feed-forward connection. Our understanding of the cortical maps interactions is that this graph has no cycle: we can not have $i \succ i$ for some i. Furthermore, with such an acyclic connections and in the *absence* of backward connections, the final result is easy to predict: given some inputs, each iterative computation in a cortical map yield a stable result and from upstream to downstream this stable result propagates. This is the case for very fast brain computation [60] where, due to very short latencies, only feed-forward computations occur.

The situation is very different when backward connections interact: several criteria are to be minimized simultaneously, yielding a apparently very complex dynamical system, with the risk of interferences, oscillations, chaotic behavior, etc.. What is the result of such interactions is also to clarify.

The proposed solution of this problem is based on the following *fact:*

minimizing, $\forall\, i$ *the criteria* $\mathcal{L}_i$ *with respect to* $\mathbf{h}_i$

is equivalent to minimize with respect to $\mathbf{h}_\bullet$*, in the general case:*

$$\mathcal{L}_\bullet = \sum_i \nu(||\nabla_i \mathcal{L}_i||)\, \mathcal{L}_i$$

writing $\nabla_i = \partial/\partial \mathbf{h}_i$. *Here,* $\nu()$ *is a* $\mathcal{R}^+ \to \mathcal{R}^+$ *positive strictly increasing profile with* $\nu(u) \geq 0$, $\nu'(u) > 0$, $\nu(0) = 0$ *and* $\lim_{u\to 0} \nu'(u)/u = 0$. *For instance* $\nu(u) = u^\alpha$ *with* $\alpha > 2$.

This criterion provides a view of what is a common objective for the different cortical maps computations.

Let us derive this *fact*:

(i) if all $\mathcal{L}_i$ are minimal with respect to $\mathbf{h}_i$, then $\nabla_i \mathcal{L}_i = 0$ thus $\nu(||\nabla_i \mathcal{L}_i||) = 0$ and $\mathcal{L}_\bullet = 0$ but $\mathcal{L}_\bullet$ is also positive as a sum of positive terms, so that 0 is its minimal value, now attained: $\mathcal{L}_\bullet$ is thus minimal.

(ii) If $\mathcal{L}_\bullet$ is minimal, its gradient vanishes, i.e. $\nabla_\bullet \mathcal{L}_\bullet = (\cdots \nabla_k \mathcal{L}_\bullet, \cdots) = 0$, writing $\nabla_\bullet = \partial/\partial \mathbf{h}_\bullet$. As a consequence:

$$\forall k \quad 0 = \nabla_k \mathcal{L}_\bullet = \textstyle\sum_i \nu(||\nabla_i \mathcal{L}_i||)\, \nabla_k \mathcal{L}_i + \nu'(||\nabla_i \mathcal{L}_i||)/||\nabla_i \mathcal{L}_i||\, \gamma_{ki}$$

writing $\gamma_{ki} = (\nabla_k \nabla_i \mathcal{L}_i)\, \nabla_i \mathcal{L}_i$. This derivation comes from the fact that $\nabla \nu(||\mathbf{g}||) = \nu'(||\mathbf{g}||)/||\mathbf{g}||(\nabla \mathbf{g})\, \mathbf{g}$ as the reader can easily verify.

Because $\lim_{u\to 0} \nu'(u)/u < +\infty$ this expression is well defined even for small $\nabla_i \mathcal{L}_i$, i.e event when closed to the optimum.

Let us rewrite this expression :

$$\forall k \quad 0 = \nabla_k \mathcal{L}_\bullet = \nu(||\nabla_k \mathcal{L}_k||)\, \nabla_k \mathcal{L}_k + \nu_k$$

with $\nu_k = \sum_{i\neq k} \nu(||\nabla_i \mathcal{L}_i||)\, \nabla_k \mathcal{L}_i + \sum_i \nu'(||\nabla_i \mathcal{L}_i||)/||\nabla_i \mathcal{L}_i||\, \gamma_{ki}$. These two vectors have a "huge" dimension $dim(\nabla_k \mathcal{L}_k) = dim(\gamma_{ki}) = dim(\vec{\mathbf{h}})$, i.e. the dimension of the map (the number of neurons). In the general case, there are independent, because γ_{ki} contains, if generic, terms which do not linearly depends on $\nabla_k \mathcal{L}_k$. As a consequence, their sum being equal to zero, both vectors must vanish so that $||\nabla_k \mathcal{L}_k||^\alpha \nabla_k \mathcal{L}_k = 0 \Rightarrow \nabla_k \mathcal{L}_k = 0$. The gradients of all $\mathcal{L}_k$ vanish, so that these convex quadratic criteria are minimized.

A step further, minimizing each criterion without considering the other criteria and parameters means from (4) as implemented in (11), applying the rule:

$$\frac{\partial \mathbf{h}_k}{\partial t} = -\nabla_k \mathcal{L}_k$$

rewritten with the present notations. Does this decreases the common criterion ?

Let us study this second fact:

From the derivation:

$$\frac{\partial \mathcal{L}_\bullet}{\partial t} = \nabla_\bullet \mathcal{L}_\bullet^T \frac{\partial \mathbf{h}_\bullet}{\partial t} = \sum_k \nabla_k \mathcal{L}_\bullet^T \frac{\partial \mathbf{h}_k}{\partial t} = -\sum_k \nabla_k \mathcal{L}_\bullet^T \nabla_k \mathcal{L}_k$$

it appears that the common criterion decreases if and only if $\sum_k \nabla_k \mathcal{L}_\bullet^T \nabla_k \mathcal{L}_k > 0$

From (4), with a few algebra:

$$\nabla_k \mathcal{L}_i = \begin{cases} \mathbf{\Lambda}_i \left[\mathbf{h}_i - \bar{\mathbf{h}}_i\right] - \Delta_{\mathbf{L}_i} \mathbf{h}_i & \text{if } k = i \\ \rho'(\bar{\mathbf{h}}_k)\, \mathbf{\Lambda}_i \left[\bar{\mathbf{h}}_i - \mathbf{h}_i\right] + \nabla_k^\epsilon \mathcal{L}_i & \text{if } \rho(\mathbf{h}_k) = \bar{\mathbf{h}}_i \\ \nabla_k^\epsilon \mathcal{L}_i & \text{otherwise} \end{cases}$$

writing $\nabla_k^\epsilon \mathcal{L}_i = \frac{1}{2}\left[\sum_{j \neq i} ||\mathbf{h}_j - \bar{\mathbf{h}}_j||^2_{\nabla_i \mathbf{\Lambda}_j} + ||\nabla \mathbf{h}_j||^2_{\nabla_i \mathbf{L}_j}\right]$.

Because of the action of the spatial smoothing operator

$$\nabla_i \mathbf{\Lambda}_j = \nabla[\mathbf{\Lambda}_j (S * \mathbf{h}_{\bullet i})] = \nabla \mathbf{\Lambda_j} (S * \mathbf{h}_{\bullet i})\, [\nabla S * \mathbf{h}_{\bullet i}]$$

has a small magnitude since, by definition, of a smoothing operator $||\nabla S||$ is small, say $||\nabla S|| = o(1/\omega)$, where ω is the smoothing filter window size (e.g. for an isotropic Gaussian filter $S(\mathbf{u}) = 1/\sqrt{2\,\Pi}/\omega e^{-\frac{1}{2}\frac{||\mathbf{u}||^2}{\omega^2}}$ the reader can easily verify that $||\nabla S|| = o(1/\omega^{1+dim(\mathbf{h})/2})$. Similarly $\nabla_i \mathbf{L}_j$ has also a small magitude. As a linear combination of small quantities, $\nabla_k \mathcal{L}_i$ is thus small and we can write $||\nabla_k^\epsilon \mathcal{L}_i|| = o(1/\omega)$, as soon as $k \neq i$ and $\rho(\mathbf{h}_k) \neq \bar{\mathbf{h}}_i$.

A step further, calculating $\nabla_k \nabla_i \mathcal{L}_i$ to evaluate γ_{ki}:

- if $k = i$,

$\nabla_k^2 \mathcal{L}_i(\mathbf{x}_u) = \frac{\partial}{\partial \mathbf{h}_k(\mathbf{x}_u)}\left[\mathbf{\Lambda}_k \left[\mathbf{h}_k - \bar{\mathbf{h}}_k\right](\mathbf{x}_u) - \sum_v \sigma_k^{uv}\, \mathbf{h}_k(\mathbf{x}_v)\right] = [\mathbf{\Lambda}_k - \sigma_k^{uu}](\mathbf{x}_u)$

As discussed previously $\sigma^{uu}(\mathbf{x}_u) < 0$ (remind that in $\Delta_{\mathbf{L}}(\mathbf{x}_u)$ we perform a weighted average around $\mathbf{x}_u$ and *subtract* the same weight at $\mathbf{x}_u$, as visible in (8)) so that the matrix $\mathbf{\Lambda}_k - \sigma_k^{uu}$ is positive.

- if $\rho(\mathbf{h}_k) = \bar{\mathbf{h}}_i$,

$$\nabla_k \nabla_i \mathcal{L}_i = \frac{\partial}{\partial \mathbf{h}_k}\left[\mathbf{\Lambda}_i \left[\mathbf{h}_i - \mathbf{h}_k\right] - \Delta_{\mathbf{L}}\, \mathbf{h}_i\right] = -\mathbf{\Lambda}_i$$

- otherwise because $\nabla_k \nabla_i \mathcal{L}_i = \nabla_i \nabla_k \mathcal{L}_i$ has an order of magnitude related to $||\nabla_k \mathcal{L}_i||$, we can simply write $||\nabla_k \nabla_i \mathcal{L}_i|| = o(1/\omega)$ as soon as $k \neq i$ and $\rho(\mathbf{h}_k) \neq \bar{\mathbf{h}}_i$.

Summarizing:

$$\gamma_{ki} = \begin{cases} [\mathbf{\Lambda}_k - \sigma_k^{uu}]\, \nabla_k \mathcal{L}_k & \text{if } k = i \\ -\mathbf{\Lambda}_i\, \nabla_i \mathcal{L}_i + o(1/\omega) & \text{if } \rho(\mathbf{h}_k) = \bar{\mathbf{h}}_i \\ o(1/\omega) & \text{otherwise} \end{cases}$$

so that:

$$\nabla_k \mathcal{L}_\bullet = \mathbf{U}_k\, \nabla_k \mathcal{L}_k + \sum_{i, \rho(\mathbf{h}_k) = \bar{\mathbf{h}}_i} \lambda_i + o(1/\omega)$$

with $\mathbf{U}_k = \nu(||\nabla_k \mathcal{L}_k||) + \nu'(||\nabla_k \mathcal{L}_k||)/||\nabla_k \mathcal{L}_k|| \, [\mathbf{\Lambda}_k - \sigma_k^{uu}]$ which is a positive definite matrix
while $\lambda_i = \nu(||\nabla_i \mathcal{L}_i||) \, \nabla_k \mathcal{L}_i - \nu'(||\nabla_i \mathcal{L}_i||)/||\nabla_i \mathcal{L}_i|| \, \mathbf{\Lambda}_i \, \nabla_i \mathcal{L}_i$ and finally:

$$\begin{aligned} \frac{\partial \mathcal{L}_\bullet}{\partial t} &= -\sum_k \nabla_k \mathcal{L}_\bullet^T \, \nabla_k \mathcal{L}_k \\ &= -\left[\sum_k ||\nabla_k \mathcal{L}_k||^2_{\mathbf{U}_k} + \sum_{ik, \rho(\mathbf{h}_k) = \bar{\mathbf{h}}_i} \lambda_i^T \, \nabla_k \mathcal{L}_k\right] + o(1/\omega) \end{aligned}$$

Clearly, without forward links (i.e. no $ik, \rho(\mathbf{h}_k) = \bar{\mathbf{h}}_i$), it appears that minimizing each criterion yields to the global minimization of the criterion, since:

$$\forall k, \frac{\partial \mathbf{h}^k}{\partial t} = -\nabla_k \mathcal{L}_k \Rightarrow \frac{\partial \mathcal{L}_\bullet}{\partial t} = -\sum_k ||\nabla_k \mathcal{L}_k||^2_{\mathbf{U}_k} < 0$$

Considering now forward links, the previous inequality is not necessarily true for $\mathcal{L}_\bullet$ because terms related to $\lambda_i^T \, \nabla_k \mathcal{L}_k$ are indeed not necessarily positive: this means that the common criterion may -at least temporarily- increase.

However, because forward links define a lattice, i.e. a graph without cycles, let us consider at time t_0 the subset $\mathbf{h}_{\bullet_0} = (\cdots \mathbf{h}_i, \cdots)$ (say a layer) of cortical maps values which do not receive any forward connection, i.e. which are only connected to inputs. This defines a sub-lattice without forward connections. The related criterion $\mathcal{L}_{\bullet_0}$ is thus strictly decreasing and reaches its minimum (up to a certain precision ϵ) after a certain delay at time, say, t_1, thanks to what as being discussed previously.

At time t_τ, $\tau = 1$, when $\mathcal{L}_{\bullet_{\tau-1}}$ is minimized, let us consider the subset $\mathbf{h}_{\bullet_\tau} = (\cdots \mathbf{h}_i, \cdots)$ (say a layer) of cortical map values which do not receive any forward connection, except from $\mathbf{h}_{\bullet_{\tau-1}}$. Because $\mathcal{L}_{\bullet_{\tau-1}}$ is already minimized, the gradients $\nabla_i \mathcal{L}_i$ of $\mathbf{h}_i$ in $\mathbf{h}_{\bullet_{\tau-1}}$ vanish and the related λ_i also vanish, as visible above. As a consequence, forward links do not influence the related criterion $\mathcal{L}_{\bullet_\tau}$ which is thus strictly decreasing and reaches its minimum (up to a certain precision ϵ) after a certain delay at time, say, $t_{\tau+1}$.

Iterating this for $\tau = 1, 2, \cdots$, $\mathbf{h}_{\bullet_0 \cdots \bullet_\tau} = \cup_\tau \mathbf{h}_{\bullet_\tau}$ is a strictly increasing set so that we must have, for a $\tau_\bullet$, $\mathbf{h}_{\bullet_0 \cdots \bullet_{\tau_\bullet}} = \mathbf{h}_\bullet$. As a consequence, at time $t_{\tau_\bullet}$ or before, the related criterion $\mathcal{L}_\bullet$ is minimized.

This demonstrates -in the worst case- the minimization of $\mathcal{L}_\bullet$: the key fact is that downstream layers do not influence upstream layers allowing minimization in these layers to be stable and the relate result to propagate.

> In practice, there is no need to "wait until" each separate minimization is achieved: realized in parallel, these minimizations are expected to be much faster.

As a consequence, the answer is positive: *minimizing each criterion without considering the other criteria and parameters also decreases the common criterion*, thanks to the biologically driven assumptions: (i) space smoothing in backward connections, (ii/iii) forward connections graph being a lattice.

This is a crucial fact, because this also means that minimizing each criterion is a convergent process, since it corresponds to a common criterion minimization. As a consequence, we have a formal verification that feedback links in our framework and with the proposed assumptions yields a well-defined process.

More than that, the previous derivation also describes qualitatively how interactions between different cortical maps occurs:
- backward connections have a constant influence in the sense that they can very rapidly tune the processing of a cortical map but do not interfere with the convergence inside a such a map, they propagate information between the cortical maps, in a stable way; very fast propagation can occur in "one step", i.e. without inducing transient effects
- forward connections act as a "data propagation" though the related lattice and may induce transient effects on downstream layers,
- if a cortical map input is changed (because the cortex inputs vary dynamically) the overall process is still convergent.

4 Conclusion

A biologically plausible implementation of differential operators based on diffusion processes as required in regularization mechanisms has been proposed. It is designed to model "vectorial" cortical map computations. An interesting extension of the present work would be to consider not only vectorial but quantities with more complex properties such as transformation groups or diffusion tensors [63], e.g. following the track initiated by [30].

This framework is an attempt to provide an implementable model of cortical maps coding vectorial quantities and computed by networks of neurons. It is based on an integral approximation of the diffusion operator as used

in regularization mechanisms, providing an optimal implementation with the interesting property that, when used as a model of biological plausible mechanisms, it corresponds to a simple local feedback defined over a small bounded region of the parametric space.

We also consider the interactions between cortical maps, and propose simple biologically plausible conditions to guaranty the stability of such interacting layers. As such, this provides a biological plausible model of cortical map computations and interactions. What appears here is that feedback mechanisms is the key issue regarding cortical map interactions.

A perspective: understanding the role of feedbacks

The roles attributed to top-down influences are numerous [8]: feedback connections are thought to be involved in directing attention, in memory retrieval, in comparing internal models with sensory inputs, in combining global and local processing. For instance:

Where to process (low-level) : simple cues allow to decide in which part of the retinal map visual processing have to occur:
- a rough but fast edge detector may be used to determine which contrasted areas have to analyzed [48],
- large scale (smoothed, eliminating noise) orientation detector may help to tune further process of visual cues (e.g. figure/background segmentation [52]),
- low-level but efficient focus of attention towards *close*, *mobile* or *textured* objects is derived from fast rotationally stabilized motion perception [67].

More generally, our capacity to dynamically focused our visual perception on a relevant part of the visual scene and to quickly react to modifications on these, may be related to feedback mechanism. One aspect of this capability (i.e. focus of attention) has been studied in computer vision (e.g. [67, 48]) although limited to low-level perception.

What to process (high-level) : very fast object recognition, as experimented and modelized by, e.g. [61, 60], allows a "model-based" processing of the visual information with the possibility to choose among memorized

previous processing modes, configurations of parameters tuned with respect to this first recognition. This is also related to "focus of attention", including consciousness [7].

Holistic perception : naive introspection shows that we are able to almost instantaneously perform the grouping of local and even random tokens or attributes (e.g. the dalmatian picture), yielding a global object perception [43]. This includes "hallucinations" of 2D or 3D shapes from partial information (e.g. the Kanizsa triangle) [26]. Holistic perception may be related to fast-brain object labelization: feedbacks from what has been detected by this "1st stage" may be the key feature of holistic perception [8].

Opportunism : One principle which seems to control all visual perception is that "the end justifies the means". This means that in order to elaborate our percepts, our brain has an extraordinary capacity to combine several attributes (color, texture, motion, stereo, etc..), but always choosing those well adapted to a given context or to a given task [48]. This occurs dynamically and without any conscious effort. Feedbacks in the visual cortex seems to be used to select the relevant attributes, given a task or context [18], as soon as this state has been either detected or input to the system by higher "layers" of the cortex or obtained from a-priori information.

Our belief is that, feedback play a fundamental role in this context. The present formalism provides a tool to model and simulate complex interactions between cortical maps. The challenge is now to simulate the perceptual behavior of the visual system, including general feedback interactions, the proposed framework being a basic tool to attain this goal.

References

[1] L. Alvarez and J. Morel. Formalization and computational aspects of image analysis. *Acta Numerica*, pages 1–59, 1994.

[2] A. Angelucci and J. Bullier. Reaching beyond the classical receptive field of V1 neurons: horizontal or feedback axons? *J. Physiol. (Paris)*, 2002.

[3] G. Aubert and P. Kornprobst. *Mathematical Problems in Image Processing: Partial Differential Equations and the Calculus of Variations*, volume 147 of *Applied Mathematical Sciences*. Springer-Verlag, Jan. 2002.

[4] G. Boyton, S. Engel, G. Glover, and D. Heeger. Linear system analysis of functional magnetic resonance imaging in human v1. *J. Neuroscience*, 16(13):4207–4221, 1996.

[5] C. Büchel and K. Friston. Modulation of connectivity in visual pathways by attention: cortical interactions evaluated with structural equation modelling and fmri. *Cereb. Cortex*, 7:768–778, 1997.

[6] G. Bugmann. Biologically plausible neural computation. *Biosystems*, 40:11–19, 1997.

[7] J. Bullier. Feedback connections and conscious vision. *Trends in Cognitive Science*, 5(9):369–370, 2001.

[8] J. Bullier. Integrated model of visual processing. *Brain Res. Reviews*, 36:96–107, 2001.

[9] Y. Burnod. *An adaptive neural network: the cerebral cortex*. Masson, Paris, 1993. 2nd edition.

[10] C. Caudek and N. Rubin. Segmentation in structure from motion: modeling and psychophysics. *Vision Research*, 41:2715–2732, 2001.

[11] P. Degond and S. Mas-Gallic. The weighted particle method for convection-diffusion equations. *Mathematics of Computation*, 53(188):485–525, 1989.

[12] R. Deriche and O. Faugeras. Les EDP en Traitement des Images et Vision par Ordinateur. *Traitement du Signal*, 13(6), 1996.

[13] R. Deriche, O. Faugeras, G. Giraudon, T. Papadopoulo, and R. Vaillant. Four applications of differential geometry to computer vision. In G. Orban and H.-H. Nagel, editors, *Artificial and Biological Vision Systems*, Basic Research Series, pages 93–141. Springer–Verlag, 1993.

[14] R. Durbin, C. Miall, and G. Mitchinson, editors. *The computing neuron*. Addison-Wesley, 1989.

[15] C. Eliasmith and C. H. Anderson. *Neural Engineering: Computation, Representation and Dynamics in Neurobiological Systems*. MIT Press, 2003.

[16] O. Faugeras. *Three-Dimensional Computer Vision: a Geometric Viewpoint*. MIT Press, 1993.

[17] D. Felleman and D. V. Essen. Distributed hierarchical processing in the primate cerebral cortex. *Cereb Cortex*, 1:1–47, 1991.

[18] K. Friston. Functional integration and inference in the brain. *Prog Neurobiol*, 68:113–143, 2002.

[19] W. Gerstner and W. M. Kistler. Mathematical formulations of hebbian learning. *Biol Cybern*, 87:404–415, 2002.

[20] M. Giese and M. Lappe. Measurement of generalization fields for the recognition of biological motion. *Vision Research*, 38:1847–1858, 2002.

[21] M. Giese and T. Poggio. Neural mechanisms for the recognition of biological movements and actions. *Nature Neuroscience*, 2003. in press.

[22] P. Girard and J. Bullier. Visual activity in area v2 during reversible inactivation of area 17 in the macaque monkey. *J. Neurophysiol.*, 62(6):1287–1301, 1989.

[23] T. Gisiger, S. Dehaene, and J. P. Changeux. Computational models of association cortex. *Curr. Opin. Neurobiol.*, 10:250–259, 2000.

[24] N. H. Goddard, M. Huckab, F. Howell, H. Cornelis, K. Shankar, and D. Beeman. Towards neuroml: Model description methods for collaborative modelling in neuroscience. *Philosophical Transactions of the Royal Society*, 356(1412):1209–1228, 2001.

[25] S. Grossberg and N. McLoughlin. Cortical dynamics of three-dimensional surface perception: binocular and half-occluded scenic images. *Neural Networks*, 10(9):1583–1605, 1997.

[26] S. Grossberg, E. Mingolla, and W. D. Ross. Visual brain and visual perception: how does the cortex do perceptual grouping? *Trends in Neurosciences*, 20(3):106–111, 1997.

[27] A. Grunewald and S. Grossberg. Self-organization of binocular disparity tuning by reciprocal cortico-geniculate interactions. *Journal of Cognitive Neuroscience*, 10:199–215, 1998.

[28] F. Guichard and J.-M. Morel. *Image analysis and P.D.E.'s.* Tutorials on Geometrically Based Motion, IPAM, Ucla, Los Angeles, 2001.

[29] G. Hermosillo. *Variational Methods for Multimodal Image Matching.* PhD thesis, INRIA, The document is accessible at ftp://ftp-sop.inria.fr /robotvis/html/Papers /hermosillo:02.ps.gz, 2002.

[30] G. Hermosillo, C. Chefd'hotel, and O. Faugeras. Variational methods for multimodal image matching. *ijcv*, 50(3):329–343, Nov. 2002.

[31] A. Hodgkin and A. Huxley. A quantitative description of membrane current and its application to conduction and excitation in nerve. *Journal of Physiology*, 117:500–544, 1952.

[32] J. J. Hopfield. Neural networks and physical systems with emergent collective computational abilities. *Proc. National Academy of Sciences, USA*, 79:2554–2558, 1982.

[33] D. Hubel. *L'oeil, le cerveau et la vision : les étapes cérébrales du traitement visuel.* L'univers des sciences. Pour la science, 1994.

[34] A. Johnston, C. Benton, and P. M. Owan. Induced motion at textured-defined motion boundaries. *Proc. R. Soc. London*, 266:2441–2450, 1999.

[35] D. M. Keefry, J. Watson, R. Frackowiak, K. Fong, and S. Zeki. The activity in human areas v1/v2, v3 and v5 during the perception of coherent and incoherent motion. *Neuroimage*, 5:1–12, 1997.

[36] J. J. Koenderink. The brain as a geometry engine. *Psychol. Res.*, 52:122–127, 1990.

[37] A. Leonard. Vortex methods for flow simulations. *J. Comput. Phys*, 37:289–335, 1980.

[38] V. Marcar, S. Raiguel, and D.-K. X. andG.A Orban. Processing of kinetically defined boundaries in v1 and v2 of the macaque monkey. *J. NeuroPhysiol*, 84:2786–2798, 2000.

[39] V. Marcar, D.-K. Xiao, S. Raiguel, H. Maes, and G. Orban. Processing of kinetically defined boundaries in the cortical motion area mt of the macaque monkey. *J. of NeuroPhysiology*, 74(3):1258–1271, 1995.

[40] M.Carandini, D.J.Heeger, and J.A.Movshon. *Linearity and gain control in V1 simple cells*, chapter 13. New York:Plenum Press, Aug. 1998.

[41] N. McLoughlin and S. Grossberg. Cortical computation of stereo disparity. *Vision Res*, 38(1):91–99, 1998.

[42] H. Nagel and W. Enkelmann. An investigation of smoothness constraint for the estimation of displacement vector fiels from images sequences. *IEEE Transactions on Pattern Analysis and Machine Intelligence*, 8:565–593, 1986.

[43] H. Neumann and E. Mingolla. Computational neural models of spatial integration in perceptual grouping. In T. . P. Kellman, editor, *From Fragments to Objects: Grouping and Segmentation in Vision*, pages 353–400. Amsterdam: Elsevier, 2001.

[44] L. Novak and J. Bullier. *The Timing of Information Transfer in the Visual System*, volume 12 of *Cerebral Cortex*, chapter 5, pages 205–241. Plenum Press, New York, 1997.

[45] S. V. Oostende, S. Sunaert, P. V. Hecke, G. Marchal, and G. A. Orban. The kinetic occipital (ko) region in man: an fmri study. *Cerebral cortex*, 7:690–701, 1997.

[46] J. Petitot and Y. Tondut. Vers une neuro-géométrie. fibrations corticales, structures de contact et contours subjectifs modaux. *Mathématiques, Informatique et Sciences Humaines*, 145:5–101, 1999.

[47] R. Raizada and S. Grossberg. Towards a theory of the laminar architecture of the cerebral cortex: Computational clues from the visual system. *Cerebral Cortex*, 13:100–113, 2003.

[48] R. Rao and D. Ballard. Predictive coding in the visual cortex: a functional interpretation of some extra-classical receptive-field effects. *Nat Neurosci*, 2(1):79–87, 1999.

[49] R. Rao and T. J. Sejnowski. Spike-timing-dependent hebbian plasticity as temporal difference learning. *Neural Comput.*, 13(10):2221–2237, 2001.

[50] P. A. Raviat. An analysis of particle methods. In F. Brezzi, editor, *Numerical Methods in Fluid Dynamics*, volume 1127 of *Lect. Notes in Math.*, pages 243–324. Springer Verlag, Berlin, 1985.

[51] K. Rockland and D. Pandya. Laminar origins and terminations of cortical connections in the occipital lobe in the rhesus monkey. *Brain Res*, 179:3–20, 1979.

[52] N. Rubin. Figure and ground in the brain. *Nature Neuroscience*, 4:857–858, 2001.

[53] N. Rubin. The role of junctions in surface completion and contour matching. *Perception*, 30:339–366, 2001.

[54] P. Salin and J. Bullier. Corticocortical connections in the visual system: structure and function. *Psychol. Bull.*, 75:107–154, 1995.

[55] J. Sandell and P. Schiller. Effect of cooling area 18 on striate cortex cells in the squirrel monkey. *J. Neurophysiol.*, 48:38–48, 1982.

[56] G. Sary, R. Vogels, G. Kovacs, and G. Orban. Responses of monkey inferior temporal neurons to luminance- motion- and texture- defined gratings. *J. of Neurophysiology*, 4:1341–1354, 1995.

[57] L. Schwartz. *Théorie des distributions*. Hermann, 1957.

[58] E. P. Simoncelli and D. Heeger. A model of neuronal responses in visual area mt. *Vision Research*, 38:743–761, 1998.

[59] S. Theodoridis and K. Koutroumbas. *Pattern Recognition*. Academic Press, 1999.

[60] S. Thorpe and M. Fabre-Thorpe. Seeking categories in the brain. *Science*, 291:260–263, 2001.

[61] S. Thorpe, D. Fize, and C. Marlot. Speed of processing in the human visual system. *Nature*, 381:520–522, 1996.

[62] A. Tikhonov. Regularization of incorrectly posed problems. *Soviet. Math. Dokl.*, 4:1624–1627, 1963.

[63] D. Tschumperlé and R. Deriche. Constrained and unconstrained PDE's for vector image restoration. In I. Austvoll, editor, *Proceedings of the 10th Scandinavian Conference on Image Analysis*, pages 153–160, Bergen, Norway, June 2001.

[64] D. Tschumperlé and R. Deriche. Vector-valued image regularization with PDE's : A common framework for different applications. In *IEEE Conference on Computer Vision and Pattern Recognition*, Madison, Wisconsin (United States), June 2003.

[65] D. Van-Essen. Organization of visual areas in macaque and human cerebral cortex. In L. Chapula and J. Werner, editors, *The Visual Neurosciences*. MIT Press, 2003.

[66] T. Viéville. Biologically plausible regularization mechanisms. RR 4625, INRIA, 2002.

[67] T. Viéville, E. Clergue, R. Enciso, and H. Mathieu. Experimentating with 3-D vision on a robotic head. *Robotics and Autonomous Systems*, 1995. 14(1).

[68] T. Vieville, D. Lingrand, and F. Gaspard. Implementing a multi-model estimation method. *The International Journal of Computer Vision*, 44(1), 2001.

[69] G. Weisbuch. *Complex systems dynamics : an introduction to automata networks*. Addison-Wesley, 1991.

[70] A. J. Yu, M. Giese, and T. Poggio. Biophysiologically plausible implementations of maximum operation. *Neural Computation*, 14(12), 2003.

[71] S. Zeki and S. Shipp. The functional logic of cortical connections. *Nature*, 335:311–316, 1988.

Acknowledgments: *Jean Bullier*, *Frédéric Alexandre* and *Olivier Faugeras* are gratefully acknowledged for some powerful ideas at the origin of this work.This work has been realized within the scope of the RIVAGe project.

Unité de recherche INRIA Sophia Antipolis
2004, route des Lucioles - BP 93 - 06902 Sophia Antipolis Cedex (France)

Unité de recherche INRIA Futurs : Parc Club Orsay Université - ZAC des Vignes
4, rue Jacques Monod - 91893 ORSAY Cedex (France)
Unité de recherche INRIA Lorraine : LORIA, Technopôle de Nancy-Brabois - Campus scientifique
615, rue du Jardin Botanique - BP 101 - 54602 Villers-lès-Nancy Cedex (France)
Unité de recherche INRIA Rennes : IRISA, Campus universitaire de Beaulieu - 35042 Rennes Cedex (France)
Unité de recherche INRIA Rhône-Alpes : 655, avenue de l'Europe - 38334 Montbonnot Saint-Ismier (France)
Unité de recherche INRIA Rocquencourt : Domaine de Voluceau - Rocquencourt - BP 105 - 78153 Le Chesnay Cedex (France)

Éditeur
INRIA - Domaine de Voluceau - Rocquencourt, BP 105 - 78153 Le Chesnay Cedex (France)
http://www.inria.fr
ISSN 0249-6399